Viscosity of Ionic Liquids: Database, Observation, and Quantitative Structure-Property Relationship Analysis

Guangren Yu, Dachuan Zhao, Lu Wen, Shendu Yang, and Xiaochun Chen
Beijing Key Laboratory of Membrane Science and Technology, Beijing University of Chemical Technology, Beijing 100029, P. R. China

DOI 10.1002/aic.12786
Published online October 31, 2011 in Wiley Online Library (wileyonlinelibrary.com).

Viscosity data for ionic liquids (ILs) are needed for the theoretical study on viscosity or for the design/development of industrial process that involves ILs; understanding the relationship between ionic structure and viscosity is also desired to more rationally design and synthesize ILs with ideal viscosity. A database for the viscosity of pure ILs and their binary/ternary mixtures with molecular compounds is created by performing a comprehensive collection from published scientific literature sources worldwide covering the period from 1970 to 2009. In this database, there are 5046 data entries, 696 ILs, 306 cations, and 138 anions. Following the database, a direct observation of the effects of ionic structure along with temperature, pressure, and impurity on the viscosity is summarized, and a quantitative structure-property relationship (QSPR) correlation is performed to understand the viscosity at a micro-electronic or molecular level. Through direct observation and QSPR, the relationship between ILs structure and viscosity is addressed. © 2011 American Institute of Chemical Engineers *AIChE J,* 58: 2885–2899, 2012
Keywords: ionic liquids, viscosity, database, QSPR

Introduction

Ionic liquids (ILs) are a new class of solvents.[1] As illustrated in Scheme 1, ILs are entirely composed of cation and anion, and this is very different from traditional organic solvents that are composed of neutral molecules. ILs have extremely low-vapor pressure and negligible volatility,[2–4] e.g., the value of vapor pressure for toluene is 447,366 Pa at 446 K, whereas it is only 0.0067 Pa for $[C_6mim][NTf_2]$.[3] Thus, the solvent loss, environment pollution, and safety concerns from ILs volatilization may be substantially reduced, comparing with conventional volatile organic solvents.[1] Coupled with some other desirable properties such as wide liquidus range, high thermal/chemical stability, excellent and adjustable solution power for organic, inorganic, and polymeric compounds, and wide electrowindows, ILs have been under intensive studies in a variety of domains, e.g., separation technology, catalysis, electrochemistry, functional materials, etc., and presented a good perspective.[5–9] This work is focused on the viscosity of ILs.

Generally, ILs are much more viscous than conventional organic solvents, and the viscosity values of most ILs are 2–3 orders of magnitude larger than organic solvents, e.g., the viscosity of toluene is only 0.6 cP at room temperature, whereas it is 70 cP for $[C_6mim][NTf_2]$[10] and even as high as 5647 cP for $[NHH,(C_2OH)_2][OAc]$[11] where $[NHH,(C_2OH)_2]^+$ is bis(hydroxyethyl)ammonium and $[OAc]^-$ is acetate. Evidently, high viscosity will give rise to some problems in chemical processing, ranging from a negative effect on power requirements and handling (dissolution, decantation, filtration, etc.) to reduction of mass- and/or heat-transfer rate in reaction and separation processes. However, highly viscous ILs are favored in some applications such as stationary phases for gas-liquid chromatography,[12] and a fixed viscosity range is generally required when ILs are used as lubricants.[13] Therefore, to prepare ILs with ideal viscosity value is certainly a necessity. In addition to determining ILs viscosity experimentally, a fundamental understanding of the relationship between viscosity and ionic structure is also necessary to more rationally design and synthesize an IL with the desired viscosity value.

Quantitative structure-property relationship (QSPR) is an effective approach to determine a quantitative relationship between the viscosity and ionic structure for ILs. Some QSPR correlations have been performed to study the properties of ILs such as melting point,[14–20] conductivity,[21,22] density,[20,23] toxicity,[24,25] surface tension,[26] and infinite dilution activity coefficient of organic solute in ILs.[27–30] A few QSPR studies on ILs viscosity were reported where limited ILs were involved.[21,22,31] In our previous work, ILs were expanded to include $[C_4mim]^+$-, $[C_2mim]^+$-, $[BF_4]^-$-, and $[NTf_2]^-$-based ILs.[32,33] Besides QSPR, some other more qualitative analyses through direct observation showed that ILs viscosity is related to the cation–anion pairing and their structural characteristics such as cationic size, length of substituted group, flexible ether oxygen on alkyl chain, anionic size, and anionic shape.[34–48] In addition, some theoretical studies using modeling and simulation were performed for ILs viscosity, e.g., Arrhenius,[37,49–53] Vogel–Tamman–

Additional Supporting Information may be found in the online version of this article.

Correspondence concerning this article should be addressed to X. Chen at chenxc@mail.buct.edu.cn.

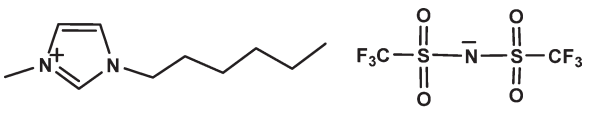

Cation Anion

Scheme 1. 1-hexyl-3-methylimidazolium bis(trifluoromethylsulfonyl)imide, [C_6mim][NTf_2].

Fulcher (VTF),[50,52–58] Litovitz,[56,57] and $(1/\eta)^{\Phi} = a + bT$ (Ref. 59) equations were used to describe the dependence of viscosity on temperature, the pressure dependence was also correlated[56,57]; Eyring's absolute rate theory with universal quasichemical activity coefficient was proved capable in describing the viscosity of binary mixtures of imidazolium-based ILs and organic solvents[60]; Stokes-Einstein and Stokes-Einstein-Debye relations were not valid for pure [C_2mim][NTf_2] and [C_2mim][NTf_2]/chloroform mixture down to the miscibility gap (at 50 wt % IL)[61]; molecular dynamic simulations[62–64] were used to calculate the viscosity of ILs or coupled with ab initio calculations[65,66] and spectrum analyses[67] to understand the relationship between the viscosity and micro-structure/-interaction, and some amine-appended imidzolium- and guanidinium-based ILs were studied by the authors.[68–72]

The viscosity data of ILs are the basic data information for the theoretical studies such as QSPR and other modeling or simulation mentioned above as well as for the design or development of an industrial process involving ILs (e.g., the calculations of heat transfer, mass transfer, and power requirements for mixing and pumping in many unit operations such as fluid transport, reactor, extraction, distillation, and heat exchanger). Therefore, data collection or database for ILs viscosity is valuable and desired. There are a few general databases or handbooks such as Merck KGaA,[73] IL Thermo,[74] CrossFire Beilstein/Gmelin,[75] and ILs database from Institute of Process Engineering, Chinese Academy of Sciences (IPE),[76] where a wide range of physicochemical properties of ILs can be found, e.g., melting point, density, surface tension, heat capacity, viscosity, etc. However, the viscosity data and other information are relatively limited. One cannot differentiate the real value from several viscosity values in different literatures if information such as ILs impurity, experimental or simulated determination method of viscosity, or ILs source (purchased or synthesized) are not provided because these factors will remarkably change the viscosity value, e.g., viscosity of ILs is sensitive to trace amounts of water and other impurities,[77,78] the viscosity of [C_4mim][NTf_2] with water content of 19 ppm is 51 cP (Ref. 79), whereas it is 27 cP (Ref. 6) with 3280 ppm water. The publication of new viscosity data over the last few years is voluminous. Therefore, a comprehensive and distinct database for the viscosity of ILs is necessary.

In this work, a viscosity database for ILs is created which includes necessary information on basics (name, ID, abbreviation, formula, molecular weight, structural formula, and CAS number), sample (sample sources, initial and final purity, purification method, and purity analysis), and viscosity (temperature, pressure, viscosity value, measurement methods or model, and reference). The viscosity data of the binary and ternary mixtures of ILs and molecular compounds are also incorporated. Following the database, some direct observations of the effect of molecular structural characteristic on the viscosity of ILs are summarized; QSPR study is performed, and the relationship between ILs structure and viscosity is illustrated. This work provides the viscosity data of ILs as data reference in theoretical study or design/development of ILs for industrial processes and sheds some light on the relationship between structure and viscosity through direct observation and QSPR.

Database

The viscosity data of ILs are generated through the following steps. (1) A search of publications on IL viscosity is performed in the science search engine of ISI web of Knowledge, the search term is "topic = ionic liquid & topic = viscosity" or "topic = ionic liquid & topic = viscosities," covering the period from 1970 to 2009, and an initial publication pool is obtained. (2) The initial publication pool is further screened to exclude publications in which no viscosity data are reported or whose data are not firsthand information but mere citations from other works. (3) The publication pool is expanded by the inclusion of new publications and references contained in the selected publications. The viscosity data are collected and tabulated from the publication pool. Three hundred and six cations, 138 anions, and 5046 data entries are finally obtained.

The database is composed of five tables (Supporting Information Tables S1–S5) and is contained in the Supporting Information.

In Supporting Information Table S1, cation and anion information are listed, which includes identification number (ID), molecular structure, full name, abbreviation, molecular formula, and molecular weight. ID contains six alphanumeric characters comprising an alphabet which represents anion or cation, followed by five numbers. For example, the ID for 1-methylimidazolium is "C01001"; the first two digitals "01" represent cation type (here is imidazolium); the last three "001" reflects the position in this type (this represents the first position), and the position is determined by molecular weight, i.e., the lower the molecular weight, the preferable the location.

In Supporting Information Tables S2–S4, the viscosity data are listed, specifically, Supporting Information Table S2 lists pure ILs, Supporting Information Table S3 contains binary system of one IL and one molecular compound, whereas Supporting Information Table S4 contains ternary system of one IL and two molecular compounds. The information includes ILs ID, CAS number, temperature, pressure, viscosity value, method of determination viscosity (exp., cal.), ILs source (synthesized by the author or commercially obtained), purity (purity of IL, impurity species, impurity content), ILs purification method, purity analysis method, and reference. In Supporting Information Table S5, the references are provided.

Results and Discussion

The studies on ILs viscosity are simply summarized in Supporting Information Figures S1–S3. The first work on ILs viscosity was reported in 1984 when Fannin et al. measured the viscosity of [C_2mim][$AlCl_4$] (17.8 cP, 298.15 K) using a viscometer[80]; after that, the viscosity values of pure 1,3-dialkylimidazolium-based ILs coupled with the fluorinated anions and binary mixture of ethylammonium nitrate and *n*-octanol are experimentally determined in 1996[39,81]; the number of studies was enhanced from 2000 as shown in Supporting Information Figure S1, although still somehow limited. Supporting Information Figure S2 indicates that more experimental studies (e.g., the measurement of ILs

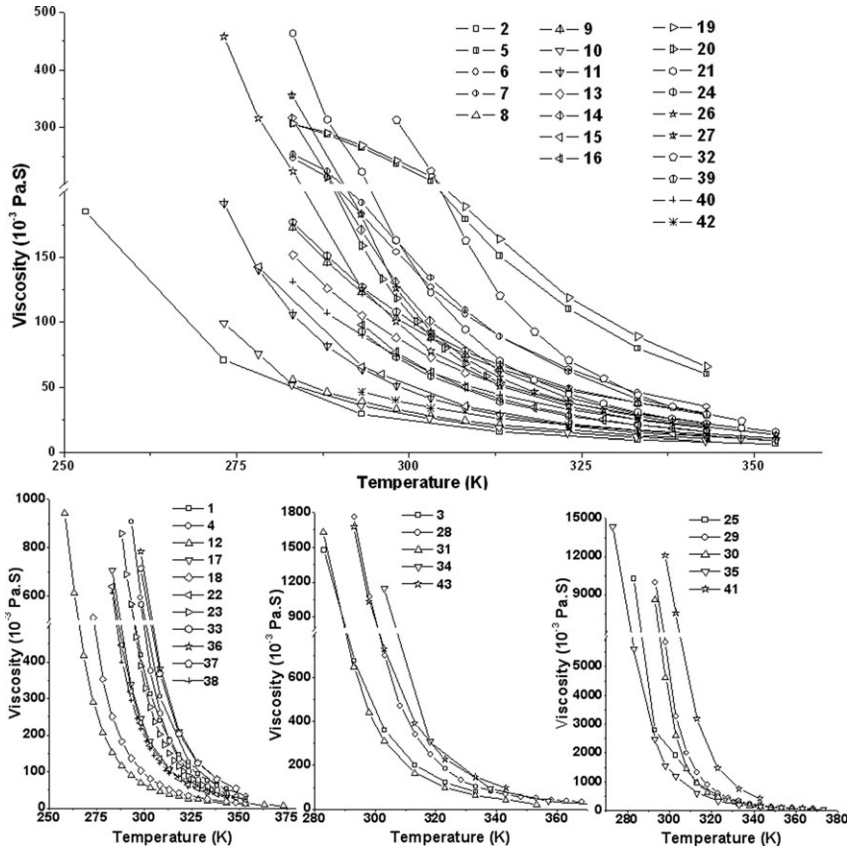

Figure 1. Viscosity of the ILs vs. temperature, refer to Table 1 for ILs numbering.

viscosity) are performed than theoretical investigation (e.g., model, simulation, or QSPR), although the studies on both the theoretical and experimental determination of ILs viscosity are relatively inadequate. Supporting Information Figure S3 gives the country distribution of the contributors.

Direct observation

Temperature. The ILs in the database, of which the viscosities are available at more than five temperature points, are selected, and their viscosities along with temperature are shown in Figure 1. For an IL, when several different viscosity values are reported at the same temperature and pressure, an average value, after eliminating aberrant values, is used for analysis, and this strategy is used in all the following analyses. As indicated in Figure 1, the viscosity of the ILs is sensitive to temperature, e.g., the viscosity sharply changes when the ILs are in lower temperatures (e.g., <300°C), the viscosity of the ILs with high viscosity values (e.g., $\sim 10^3$ cP) is especially sensitive to temperature. Such a sensitivity of ILs viscosity to temperature has been indicated in other literatures.[56–59]

The more quantitative description for the temperature dependence of viscosity of the ILs is performed using some proposed correlation equations of Arrhenius ($\eta = \eta_0 \exp(A/T)$), VTF ($\eta = \eta_0 \exp[B/(T - T_0)]$), Litovitz ($\eta = A \exp(B/RT^3)$) and $(1/\eta)^{\Phi} = a + bT$, and the results are presented in Supporting Information Tables S6–S9. As shown in Supporting Information Tables S6–S9, the numbers of the entry with $R^2 < 0.99$ (which are labeled in italics in the tables) are 5, 4, 5, and 3 for these four equations, respectively; all the equations do not present good correlations ($R^2 < 0.99$) for [N111,3OCl][NTf_2], [S11,$CH_2COOC_2H_5$][NTf_2], and [C_4C_1mim][BF_4]; to clear the effects of the functional group of cation on the exactness of correlation equations is difficult, e.g., the ILs with —COO on cation cannot be correlated well by these four equations, whereas some ILs with one group on the cation such as —O, —OH, —C=C, —C≡N, and —NH_2 is only correlated well by some equations.

A four-order polynomial correlation is proposed to describe the temperature dependence of viscosity for the ILs, and the results are shown in Table 1. It is found that the polynomial gives the satisfying correlations for all ILs with $R^2 > 0.99$ except [$P_{666,14}$][Cl] ($R^2 = 0.97621$).

Pressure. When compared with temperature, the viscosity data of ILs under different pressures are less reported. The viscosity along with pressure for ILs is shown in Figure 2, where only the values at 323.15 K are presented because it contains the most data at the temperature point. As shown in Figure 2, the viscosity increases with the pressure; the viscosities of [C_4mim][PF_6], [C_6mim][PF_6], [C_8mim][BF_4], and [C_8mim][PF_6] are more sensitive to pressure than [C_4mim][BF_4] and [C_4mim][NTf_2]. The equations such as VTF, Tait-form, Litovitz, and their modified versions have been used to quantitatively describe the pressure dependence of viscosity of [C_4mim][NTf_2], [C_4mim][PF_6], [C_4mim][BF_4], [C_6mim][NTf_2], [C_6mim][PF_6], [C_8mim][PF_6], and [C_8mim][BF_4], with good fitting of standard uncertainty < 2%.[56,57,79,82] The correlation ability of these equations is not repeatedly investigated for the viscosity data in our database, because the viscosity data under different pressures in this database are the same as those in the above studies. Here, a new three-parameter exponential equation is

Table 1. Correlation of Four-order Polynomial of $\eta = A_0 + A_1T + A_2T^2 + A_3T^3 + A_4T^4$, for Temperature Dependence of Viscosity of the ILs

No.	ILs	A_0	A_1	A_2	A_3	A_4	R^2	Number of Data Point	Temperature (K)
1	$[P_{666,14}][DCA]$	1.26*E*6	−1.52*E*4	6.83*E*1	−1.37*E* − 1	1.00*E* − 4	0.99997	11	293–343
2	$[S_{133}][DCA]$	5.98*E*4	−7.33*E*2	3.38	−6.92*E* − 1	5.31*E* − 6	0.99998	6	253–353
3	$[N_{1888}][NTf_2]$	1.27*E*7	−1.63*E*5	7.81*E*2	−1.67	1.33*E* − 3	0.99943	8	273–333
4	$[N_{4446}][NTf_2]$	7.46*E*6	−9.13*E*4	4.19*E*2	−8.53*E* − 1	6.50*E* − 4	0.99946	7	278–353
5	$[N_{111},3OCl][NTf_2]$	−3.48*E*5	4.41*E*3	−2.08*E*1	4.30*E* − 2	−3.38*E* − 5	0.99995	10	283–343
6	$[N_{111,}(CH_2)_2OOCCH_3][NTf_2]$	−1.18*E*5	1.60*E*3	−7.97	1.25*E* − 2	−1.42*E* − 5	0.99987	10	283–343
7	$[S_{11},CH_2COOC_2H_5][NTf_2]$	−2.28*E*5	2.98*E*3	−1.44*E*1	3.10*E* − 2	−2.47*E* − 5	0.99982	10	283–343
8	$[S_{222}][NTf_2]$	3.80*E*4	−4.55*E*2	2.05	−4.13*E* − 3	3.12*E* − 6	0.99971	10	283–343
9	$[S_{11},CH_2C[tbond]CH][NTf_2]$	3.79*E*4	−4.02*E*2	1.60	−2.79*E* − 3	1.82*E* − 6	0.99996	10	283–343
10	$[C_2mim][NTf_2]$	1.60*E*5	−2.01*E*3	9.43	−2.00*E* − 2	2.00*E* − 6	0.99690	9	273–343
11	$[C_4mim][NTf_2]$	1.83*E*5	−2.24*E*3	1.03*E*1	−2.00*E* − 2	2.00*E* − 5	0.99937	14	273–353
12	$[C_6mim][NTf_2]$	5.18*E*5	−6.34*E*3	2.91*E*1	−5.90*E* − 2	4.00*E* − 5	0.99012	20	258–373
13	$[C_4C_1mim][NTf_2]$	4.13*E*4	−4.48*E*2	1.82	−3.27*E* − 3	2.20*E* − 6	0.99997	10	283–343
14	$[C_6C_1mim][NTf_2]$	5.50*E*5	−6.71*E*3	3.08*E*1	−6.30*E* − 2	5.00*E* − 5	0.99985	8	283–343
15	$[C_1(2o2)pyr][NTf_2]$	1.21*E*5	−1.45*E*3	6.52	−1.30*E* − 2	9.84*E* − 6	0.99972	7	278–353
16	$[C_4C_1pyr][NTf_2]$	1.65*E*5	−1.97*E*3	8.90	−1.80*E* − 2	1.00*E* − 5	0.99998	11	283–343
17	$[C_6^2C_2^3C_1^5C_1py][NTf_2]$	1.79*E*6	−2.20*E*4	1.02*E*2	−2.10*E* − 1	1.60*E* − 4	0.99974	8	283–343
18	$[C_4mim][BF_4]$	6.28*E*5	−7.71*E*3	3.55*E*1	−7.03*E* − 2	6.00*E* − 5	0.99873	15	273–353
19	$[C_4C_1mim][BF_4]$	−2.65*E*5	3.33*E*3	−1.56*E*1	3.20*E* − 2	−2.50*E* − 5	0.99997	10	283–343
20	$[iC_{=4}mim][BF_4]$	9.84*E*5	−1.26*E*4	6.10*E*1	−1.31*E* − 1	1.10*E* − 3	0.99998	10	283–313
21	$[C_4py][BF_4]$	8.15*E*5	−9.83*E*3	4.44*E*1	−8.94*E* − 2	7.00*E* − 5	0.99310	15	283–353
22	$[C_8py][BF_4]$	1.08*E*6	−1.31*E*4	5.93*E*1	−1.19*E* − 1	9.00*E* − 5	0.99938	15	283–353
23	$[C_4^2C_1py][BF_4]$	3.65*E*6	−4.51*E*4	2.09*E*1	−4.31*E* − 1	3.30*E* − 4	0.99969	20	288–338
24	$[C_1mim][C_1SO_4]$	1.38*E*4	−1.64*E*3	7.34	−1.50*E* − 2	1.00*E* − 5	0.99997	7	293–343
25	$[N_{1,13,}(C_2OC_2OH)_2][C_1SO_4]$	2.89*E*7	−3.55*E*5	1.63*E*3	−3.35	2.57*E* −3	0.99988	7	283–343
26	$[C_2mim][C_2SO_4]$	6.89*E*5	−8.55*E*3	3.98*E*1	−8.20*E* − 2	6.00*E* − 5	0.99867	10	273–353
27	$[C_2py][C_2SO_4]$	6.41*E*5	−7.78*E*3	3.54*E*1	−7.20*E* − 2	5.00*E* − 5	0.99988	12	283–343
28	$[C_2^2CNpy][C_2SO_4]$	4.42*E*6	−5.19*E*4	2.29*E*2	−4.47*E* − 1	3.30*E* − 4	0.99581	16	293–368
29	$[C_2^3CNpy][C_2SO_4]$	3.08*E*7	−3.63*E*5	1.60*E*3	−3.14	2.00*E* − 2	0.99546	16	293–368
30	$[C_2^4CNpy][C_2SO_4]$	3.01*E*7	−3.55*E*5	1.57*E*3	−3.08	2.27*E* − 3	0.99253	16	293–368
31	$[C_4mim][OAc]$	4.19*E*6	−5.11*E*4	2.33*E*2	−4.70*E* − 1	3.60*E* − 4	0.99841	9	283–353
32	$[N_{HHH},C_2OH][OAc]$	1.00*E*6	−1.20*E*4	5.34*E*1	−1.10*E* − 1	8.00*E* − 5	0.99996	11	298–348
33	$[N_{HH},(C_2OH)_2][OAc]$	2.69*E*6	−3.22*E*4	1.45*E*2	−2.90*E* − 1	2.00*E* − 4	0.99979	11	298–348
34	$[C_{=3}mim][Cl]$	2.14*E*6	−2.38*E*4	9.93*E*1	−1.80*E* − 1	1.30*E* − 4	0.99824	6	303–394
35	***[P₆₆₆,₁₄][Cl]***	***8.12E7***	***−1.01E6***	***4.68E3***	***−9.63***	***7.40E − 3***	***0.97621***	***14***	***253–373***
36	$[P_{444},C_3NH_2][Ala]$	3.17*E*6	−3.79*E*4	1.70*E*2	−3.40*E* − 1	2.50*E* − 4	0.99995	6	298–348
37	$[P_{444},C_3NH_2][Gly]$	2.25*E*6	−2.68*E*4	1.19*E*2	−2.40*E* − 1	1.80*E* − 4	0.99998	6	298–348
38	$[C_4mim][PF_6]$	1.26*E*6	−1.53*E*4	6.96*E*1	−1.40*E* − 1	1.10*E* − 4	0.99732	16	283–353
39	$[C_4mim][SbF_6]$	2.54*E*4	−2.48*E*2	8.79*E* − 1	−1.33*E* − 3	6.90*E* − 7	0.99993	10	283–343
40	$[C_4mim][TfO]$	5.07*E*4	−5.71*E*2	2.42	−4.55*E* − 3	3.21*E* − 6	0.99983	10	283–343
41	$[N_{4444}][doc]$	8.83*E*7	−1.07*E*6	4.86*E*3	−9.83	7.45*E* − 3	0.99991	6	298–343
42	$[C_3C_1pyr][FSI]$	1.61*E*4	−1.76*E*2	7.20*E* − 1	−1.00*E* − 3	8.82*E* − 7	0.99985	8	293–353
43	$[C_4mim][C_5H_{11}O_2SO_4]$	1.33*E*7	−1.64*E*5	758.24	−1.56	1.20*E* − 3	0.99975	8	283–343

The bold italic row in the table is used for emphasis to the statement: $R^2 > 0.99$ except $[P_{666,14}][Cl]$ ($R^2 = 0.97621$).

proposed to correlate the pressure dependence of ILs viscosity at a constant temperature, $\eta = C_0 + C_1 \exp(P/b)$, and the results are shown in Table 2. As shown in Table 2, the equation gives a very good fitting with $R^2 > 0.999$.

Cation. Length of alkyl side chain, type of cation ring, and addition of characteristic atom/group are used to investigate the effects of cation on viscosity of the ILs.

As indicated in Figure 3, the viscosities of ILs generally increase with the length of alkyl side chain, which is ascribed to the fact that increasing the length of alkyl side chain will increase van der Waals interaction and thus the viscosity.[39,41,43] However, there is somewhat different for ethyl group (i.e., $n = 2$), e.g., $\eta([C_1mim][NTf_2])/44$ cP > $\eta([C_2mim][NTf_2])/37$ cP, $\eta([C_1mim][CF_3BF_3])/27$ cP > $\eta([C_2mim][CF_3BF_3])/26$ cP, $\eta([C_1mim][C_2F_5BF_3])/33$ cP > $\eta([C_2mim][C_2F_5BF_3])/27$ cP, and this may be due to a more flexibility of ethyl than methyl (i.e., more conformational degrees of freedom, which may partly compensate the van der Waals interaction).

The effects of cationic ring/core on the viscosity are shown in Supporting Information Table S10 and Figure 4. As indicated in Supporting Information Table S10, with the

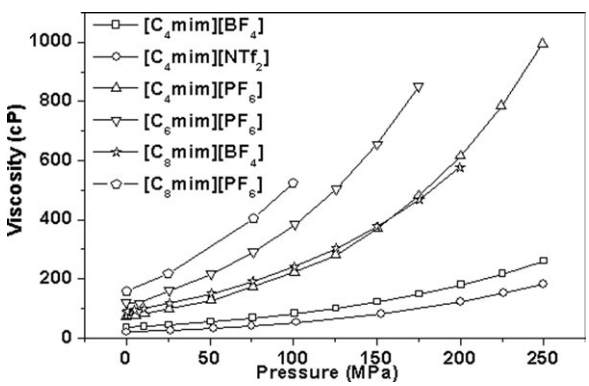

Figure 2. Viscosity of ILs vs. pressure at 323.15 K.

Table 2. Correlation of $\eta = C_0 + C_1\exp(P/b)$ for Pressure Dependence of Viscosity of the ILs

ILs	T (K)	C_0	C_1	b	R^2	Number of Data Point	Pressure (MPa)
$[C_4mim][BF_4]$	298	−19.870 ± 1.006	127.963 ± 0.841	107.450 ± 0.354	1	10	0.1–175.4
	323	−9.599 ± 0.304	45.338 ± 0.241	140.021 ± 0.352	1	12	0.1–250.1
	348	−6.070 ± 0.197	22.055 ± 0.159	177.070 ± 0.625	0.99999	14	0.1–300
$[C_4mim][NTf_2]$	298	−13.615 ± 0.634	64.406 ± 0.534	101.457 ± 0.436	1	7	0.1–150.2
	323	−7.960 ± 0.982	28.409 ± 0.757	130.985 ± 1.557	0.99996	9	0.1–249.6
	348	−5.351 ± 0.118	16.015 ± 0.092	165.116 ± 0.444	0.99999	15	0.1–298.9
$[C_4mim][PF_6]$	298	−31.562 ± 8.800	306.490 ± 6.237	79.650 ± 0.670	0.99996	11	0.1–174.1
	323	−18.461 ± 3.068	91.324 ± 2.179	103.468 ± 0.965	0.99991	15	0.1–249.3
	343	−10.190 ± 0.499	45.209 ± 0.443	122.022 ± 0.653	0.99999	11	0.1–172.9
$[C_6mim][PF_6]$	313	−46.307 ± 1.008	242.567 ± 0.838	89.327 ± 0.151	1	8	0.1–150.0
	323	−40.850 ± 9.669	154.799 ± 7.811	99.884 ± 2.340	0.99982	9	0.1–174.8
	348	−17.546 ± 0.882	58.738 ± 0.691	125.000 ± 0.662	0.99999	8	0.1–238.5
$[C_8mim][BF_4]$	298	−93.074 ± 2.314	433.346 ± 2.040	96.518 ± 0.257	1	10	0.1–117.5
	308	−67.926 ± 3.171	255.774 ± 2.668	109.291 ± 0.538	0.99998	12	0.1–200.1
	323	−35.681 ± 1.379	124.266 ± 1.200	125.146 ± 0.620	0.99999	12	0.1–199.8
	333	−25.047 ± 0.665	82.55577 ± 0.571	135.976 ± 0.497	1	10	0.1–200.0
	348	−16.841 ± 0.424	49.459 ± 0.386	154.710 ± 0.661	0.99999	15	0.1–224.2
$[C_8mim][PF_6]$	333	−33.548 ± 2.890	131.266 ± 2.629	107.494 ± 1.269	0.99999	7	0.1–125.2
	343	−18.971 ± 4.924	82.604 ± 4.049	111.887 ± 2.756	0.99987	8	0.1–175.9

same anions such as $[NTf_2]^-$, $[CF_3BF_3]^-$, $[BF_4]^-$, and $[C_2F_5BF_3]^-$, the viscosity values of the ILs with different cations follow the order: $[im]^+ < [py]^+ < [pyr]^+ < [ox]^+ < [pip]^+ < [mo]^+$; further, the viscosity values of the ILs with six-member ring cation are larger than that of the ILs with five-member ring cation, e.g., $[py]^+ > [im]^+$, $[pip]^+ > [pyr]^+$, $[mo]^+ > [ox]^+$, which has been indicated in other literatures[35,36]; the viscosity values of the ILs with nonaromatic cation are larger than that of the ILs with aromatic cation, e.g., $[pip]^+ > [py]^+$, $[mo]^+ > [py]^+$, $[pyr]^+ > [im]^+$, $[ox]^+ > [im]^+$, which may be ascribed to the more delocalized positive charge on aromatic cation and thus the weaker cation–anion interaction. As shown in Figure 4, the viscosity values of the phosphonium-based ILs with phosphorus atom on cationic center are lower than that of the ammonium-based ILs with nitrogen atom on cationic center, although the atomic weight of phosphorus is larger than that of nitrogen, as has been found.[35,44]

The effects on viscosity of characteristic atom/group on cation are presented in Table 3. As indicated in Table 3, with the exception of the alkyl ether of —OR, all the other atoms or groups such as —OH, —SR, —COOH, —C≡N, and —F will increase the viscosity. The ILs with alkyl ether on cation generally have lower viscosity, which has been ascribed to a more flexible rotation by virtue of the increase of conformational degrees of freedom.[35,36,40,43–45] The increase of ILs viscosity from the remaining characteristic atoms/groups may be contributed to the added interaction (e.g., hydrogen bond and van der Waals) between cation and anion; the strong ionic-type hydrogen bonding interaction through characteristic

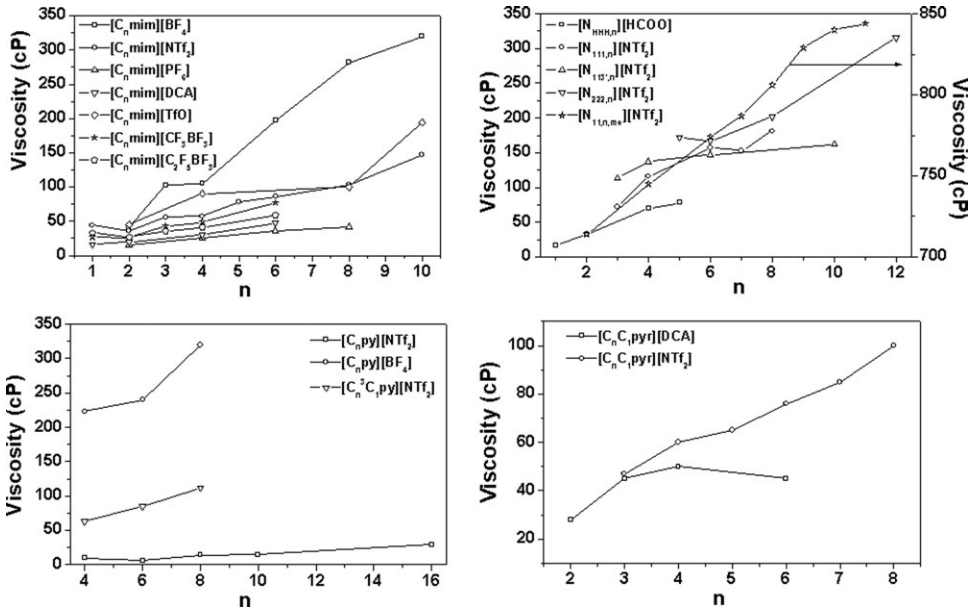

Figure 3. Effects of the length of alkyl chain in cation on ILs viscosity, and the viscosities of $[C_nmim][NTf_2]$, $[C_nmim][TfO]$, and $[C_npy][BF_4]$ are at 293 K; $[C_nmim][BF_4]$, $[C_nmim][DCA]$, $[C_nmim][CF_3BF_3]$, $[C_nmim][C_2F_5BF_3]$, $[N_{111,n}][NTf_2]$, $[N_{HHH,n}][HCOO]$, $[N_{222,n}][NTf_2]$, $[N_{113',n}][NTf_2]$, $[C_nC_1pyr][DCA]$, and $[C_n{}^3C_1py][NTf_2]$ at 298 K; $[N_{11,n,me}][NTf_2]$ and [CnC1pyr][NTf2] at 303 K; $[C_nmim][PF_6]$ and $[C_npy][NTf_2]$ at 353 K.

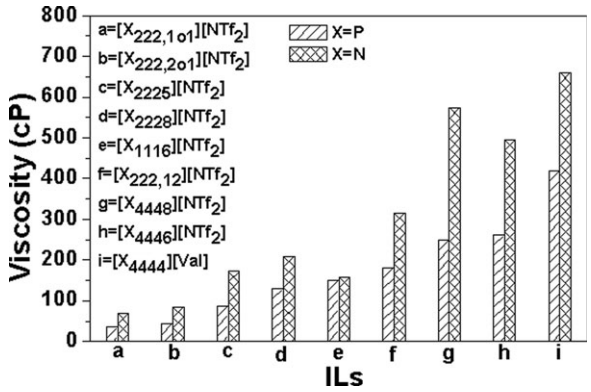

Figure 4. The viscosity of ammonium-based and phosphonium-based ILs (in cP at 298 K).

atom/group on cation and anion can dramatically increase the ILs viscosity, as demonstrated for amine-appended imidazolium and guanidinium ILs through ab initio calculations and molecular dynamics simulations by us.[68,70] Fluorinated cation is taken as one example: $[(2oC_1(CF_2)_3CHF_2)C_1mo][NTf_2]$ (970 cP at 298.15 K) vs. $[(2o5)C_1mo][NTf_2]$ (223 cP at 298.15 K), $[CF_3CH_2mim][NTf_2]$ (248 cP at 298.15 K) vs. $[C_2mim][NTf_2]$ (38.6 cP at 298.15 K), and the fluorination of cation tends to increase the viscosity due to an increase of cationic size and interionic van der Waals interaction.[39,46]

Anion. Anion type, anion size, and fluorination of the alkyl chain in anion are used to investigate the effects of anion on viscosity of the ILs, and the results are presented in Supporting Information Table S11, Tables 4 and 5, respectively.

As indicated in Supporting Information Table S11, the viscosity values of the ILs with a shared cation increase in order of $[DCA]^- < [NTf_2]^- < [TfO]^- < [BF_4]^- < [PF_6]^- < [OAc]^-$. The lower viscosity of the ILs with $[DCA]^-$ and $[NTf_2]^-$ anions is understood by the more delocalized negative charge distribution on the anion and the weaker cation–anion charge interaction to which it leads[36,41–43,45]; whereas the higher viscosity for $[BF_4]^-$ and $[PF_6]^-$ anion is ascribed to the more rigid characteristic and the lack of conformational degrees of freedom.[36,45] $[OAc]^-$ anion has the highest viscosity due to the localization of negative charge on —COO of $[OAc]^-$ and the strong hydrogen bonding and electrostatic interaction, as illustrated by the authors for [tmg][L-lactate] where $[tmg]^+$ is 1,1,3,3-tetramethylguanidinium.[70]

As indicated in Table 4, the anion size will increase the viscosity of the ILs in the same anion series because of the increased van der Waals interaction. However, it is not the case with $[BF_4]^-$-based ILs, and the viscosity values of these ILs are much higher than those of other ILs with $[C_nF_{2n+1}BF_3]^-$ (n = 1–4). Taking the ILs of $[(2o1)C_1ox][C_nF_{2n+1}BF_3]$ (n = 0–4) as typical examples, the viscosity of $[(2o1)C_1ox][BF_4]$ is 704 cP at 298 K, whereas the viscosity values of the other ILs of $[(2o1)C_1ox][C_nF_{2n+1}BF_3]$ (n = 1–4) are less than 177 cP. The high viscosity of $[(2o1)C_1ox][BF_4]$ can be understood from the fact that the effects of the rigid nature of $[BF_4]^-$ anion on viscosity with less configuration freedom surpass the effects of van der Waals interaction.[36,43,45] Besides $[BF_4]^-$, it is worth noting that the viscosity values are not linearly increasing with anion size and $[(2o1)C_1ox][C_2F_5BF_3]$ possesses the lowest viscosity. The viscosity of $[(2o1)C_1ox][C_2F_5BF_3]$ is lower than that of $[(2o1)C_1ox][CF_3BF_3]$ (which can be attributed to more configuration freedom degrees of the former than the latter, and the decreased Coulombic forces from the improved charge distribution[36,37,43,45]), whereas the viscosity values of $[(2o1)C_1ox][C_3F_7BF_3]$ and $[(2o1)C_1ox][C_4F_9BF_3]$ are higher than that of $[(2o1)C_1ox][CF_3BF_3]$ (which can be attributed to the increased van der Waals interaction for $[(2o1)C_1ox][C_3F_7BF_3]$ and $[(2o1)C_1ox][C_4F_9BF_3]$ due to increasing the length of alkly chain[36,39,43,45]). Such trends are true for the other ILs with the anions of $[C_nF_{2n+1}BF_3]$ (n = 0–4).

As indicated in Table 5, the fluorinated anion generally results into lower viscosity, and this may be ascribed to an improved charge distribution and thus the weakness of interionic electrostatic (including possible hydrogen bonding) interaction.[37,43]

Impurity. The effects of water and chloride content on ILs viscosity are presented in Supporting Information Tables S12 and S13 in Supporting Information, respectively. As indicated in Supporting Information Table S12, the viscosity values of the ILs decrease with increasing water content in the ILs; whereas the increased water content results into a higher viscosity for [C4mim][OAc], e.g., it is 139.7 cP at the water content of 746 ppm, whereas it is 440 cP at 11,003 ppm, and the reason might be the stronger interaction between water and —COO of $[OAc]^-$ than that and other anions such as $[BF_4]^-$, $[PF_6]^-$, and $[NTf_2]^-$ (in which there are delocalized negative charge distribution). Moreover, the effects on viscosity are not too remarkable when the water content is $< \sim 10^3$ ppm, whereas it is remarkable when the water content is $> \sim 10^4$ ppm. It should be noted that water content offers a great effect on the viscosity of [C6mim][Cl], e.g., it is 18,089 cP at the water content of 480 ppm, whereas it is 716 cP at 1130 ppm. As indicated in Supporting Information Table S13, the chloride content also gives a remarkable effect on the ILs viscosity. An increased chloride content generally makes the IL become more viscous. The viscosity data of some selected binary systems of ILs and other molecular compounds are illustrated in Figure 5. As indicated in Figure 5, the addition of other solutes will remarkably reduce the ILs viscosity.

It is fair to say that the aforementioned observations for the effect of cationic/anionic structural characteristics, such as the length of cationic alkyl side chain, type of cation ring, addition of characteristic atom/group to cation, anion type, anion size, and fluorination of anionic alkyl on ILs viscosity are qualitative and require further studies with quantum mechanics,[65,66,68,70] molecular dynamic simulation,[62–64,68–72] and other necessary spectrum analyses to provide quantitative evidence from the molecular viewpoint.

QSPR study

Data Set for QSPR. As presented in the database, the viscosity data are relatively limited for a class of ILs with some shared cation or anion at some temperature. For a fixed cation or anion at a constant temperature, $[C_4mim]^+$-, $[C_2mim]^+$-, $[P_{444},C_3NH_2]^+$-, $[NTf_2]^-$-, $[BF_4]^-$-, and $[DCA]^-$-based ILs have the most entries of viscosity data, making these ILs favorable for QSPR study. Among them, $[C_4mim]^+$-, $[C_2mim]^+$-, $[NTf_2]^-$-, and $[BF_4]^-$-based ILs have been studied previously.[22,32,33] So, only $[P_{444},C_3NH_2]^+$- and $[DCA]^-$-based ILs are selected to undergo the QSPR

Table 3. Viscosity Comparison between the ILs with Characteristic Atom/Group on Cation and Those Without Characteristic Atom/Group (in cP at 298 K)

Characteristic Atom/Group	ILs with Characteristic Atom/Group	Viscosity	ILs Without Characteristic Atom/Group	Viscosity
—OH	$[C_2OHmim][NTf_2]$	91	$[C_2mim][NTf_2]$	37
	$[CH_3CH(OH)CH_2mim][PF_6]$	319	$[C_4mim][PF_6]$	213
	$[CH_3CH(OH)CH_2mim][NTf_2]$	342	$[C_4mim][NTf_2]$	45
	$[CH_3CH(OH)CH_2mim][NO_3]$	502	$[C_4mim][NO_3]$	266
	$[N_{HH},(C_2OH)_2][PO_2(C_4O)_2]$	2409	$[N_{22HH}][PO_2(C_4O)_2]$	201
	$[N_{HH},(C_2OH)_2][HCOO]$	494	$[N_{22HH}][HCOO]$	5.4
	$[N_{HHH},C_2OH][HSO_4]$	309	$[N_{2HHH}][HSO_4]$	128
	$[N_{HHH},C_2OH][Lac]$	1324	$[N_{2HHH}][Lac]$	803
	$[N_{HHH},C_2OH][NO_3]$	113	$[N_{2HHH}][NO_3]$	32
	$[N_{HHH},C_2OH][HCOO]$	220	$[N_{2HHH}][HCOO]$	32
	$[C_2OHC_1pyr][NTf_2]$	80	$[C_3C_1pyr][NTf_2]$	63
	$[CH_3CH(OH)CHOHC_1pyr][NTf_2]$	1500	$[C_3C_1pyr][NTf_2]$	63
			$[C_4C_1pyr][NTf_2]$	74
	$[N_{113'},C_2OH][NTf_2]$	211	$[N_{1133'}][NTf_2]$	113
—OR	[(2o2o1)mim][Cl]	613*	$[C_6mim][Cl]$	7826*
	$[(2o2o1)mim][PF_6]$	426*	$[C_6mim][PF_6]$	680*
	$[(2o2o1)mim][BF_4]$	377*	$[C_6mim][BF_4]$	224*
	$[(2o2o1)mim][C_2F_5BF_3]$	51	$[C_6mim][C_2F_5BF_3]$	59
	$[(2o2o1)mim][CF_3BF_3]$	62	$[C_6mim][CF_3BF_3]$	77
	$[C_1(2o1)pyr][CF_3BF_3]$	87	$[C_4C_1pyr][CF_3BF_3]$	137
	$[C_1(2o1)pyr][C_2F_5BF_3]$	52	$[C_4C_1pyr][C_2F_5BF_3]$	71
	$[C_1(2o1)pyr][NTf_2]$	53	$[C_3C_1pyr][NTf_2]$	63
			$[C_4C_1pyr][NTf_2]$	74
	$[C_1(2o2)pyr][NTf_2]$	60	$[C_4C_1pyr][NTf_2]$	74
	$[(2o1)C_1pip][CF_3BF_3]$	203	$[C_4C_1pip][CF_3BF_3]$	456
	$[(2o1)C_1pip][NTf_2]$	102	$[C_3C_1pip][NTf_2]$	150
			$[C_4C_1pip][NTf_2]$	182
	$[N_{111},2o2o1][NTf_2]$	63	$[N_{1116}][NTf_2]$	153
	$[N_{HHH},2o1][HCOO]$	38	$[N_{4HHH}][HCOO]$	70
	$[(2o1)C_1mo][NTf_2]$	310	$[C_4C_1mo][NTf2]$	532
	$[(2o1)C_1mo][CF_3BF_3]$	471	$[C_4C_1mo][CF_3BF_3]$	1035
	$[(2o1)C_1mo][C_2F_5BF_3]$	260	$[C_4C_1mo][C_2F_5BF_3]$	466
	$[(2o1)C_1ox][CF_3BF_3]$	134	$[C_4C_1ox][CF_3BF_3]$	165
	$[(2o1)C_1ox][C_2F_5BF_3]$	90	$[C_4C_1ox][C_2F_5BF_3]$	108
	$[(2o1)C_1ox][BF_4]$	704	$[C_4C_1ox][BF_4]$	731
	$[(2o1)C_1ox][NTf_2]$	117	$[C_4C_1ox][NTf_2]$	145
—SR	$[C_2Smim][NTf_2]$	94	$[C_2mim][NTf_2]$	37
	$[C_4Smim][NTf_2]$	98	$[C_4mim][NTf_2]$	45
	$[C_2Smim][TfO]$	145	$[C_2mim][TfO]$	45
	$[C_4Smim][TfO]$	152	$[C_4mim][TfO]$	76
—COOH	$[C_3COOHmim][CH_3CH(BF_3)CH_2CN]$	3047*	$[C_4mim][CH_3CH(BF_3)CH_2CN]$	101*
—C≡N	$[C_3CNmim][BF_4]$	230	$[C_3mim][BF_4]$	103
			$[C_4mim][BF_4]$	112
	$[C_4CNmim][BF_4]$	553	$[C_4mim][BF_4]$	112
			$[C_6mim][BF_4]$	174
	$[C_4CNmim][PF_6]$	2181	$[C_4mim][PF_6]$	213
			$[C_6mim][PF_6]$	585
	$[C_4CNmim][Cl]$	5222	$[C_6mim][Cl]$	716
	$[C_2{}^3CNpy][C_2SO_4]$	5839	$[C_2{}^3C_1py][C_2SO_4]$	150
	$[C_4{}^3CNpy][NTf_2]$	1031	$[C_4{}^3C1py][NTf_2]$	56
			$[C_6{}^3C1py][NTf_2]$	85
—F	$[C_2F_3mim][NTf_2]$	248	$[C_2mim][NTf_2]$	36
	$[N_{1224}F][NTf_2]$	774	$[N_{1224}][NTf_2]$	161
	$[C_1,CH_2CH_2OCH_2(CF_2)_3CHF_2mo][NTf_2]$	970	$[(2o5)C_1mo][NTf_2]$	223

*At 293 K.

study, where $[P_{444},C_3NH_2]^+$ is tributyl-(3-amino-propyl) phosphonium and $[DCA]^-$ is dicyanamide. The viscosity data for $[DCA]^-$-based ILs (Set A, 23 data entries, at 298 K) and $[P_{444},C_3NH_2]^+$-based ILs (Set B, 19 data entries, at 348 K) are shown in Table 6; in each dataset, two viscosity entries are selected as model testing-data, and the others are training-data.

Computational Methods. Ab initio quantum mechanical calculations are performed with Gaussian 03.[83] Geometric optimization and thermodynamic parameters are calculated at RHF/6-31G** level. Partial atomic charges are obtained using the natural bond orbital method. Following the ab initio results, CODESSA 2.7.2 package is used to derive the correlation equations between descriptor and viscosity.[84] A detailed description for obtaining QSPR correlation equations using CODESSA package can be found in the previous work of the authors.[32] The results of R^2 vs. parameter number are shown in Figure 6, where the ordinate is the square of the correlation coefficient (R^2) and the abscissa is the number of descriptor in correlation equation. As indicated in Figure 6, four-parameter correlation equation is adopted for both the two sets.

Table 4. Viscosity Comparison Among the ILs with Different Size of Anion (in cP)

Cation	Anion	T (K)	Viscosity	Cation	Anion	T (K)	Viscosity
$[C_2mim]$	[TA]	293.15	35	[Hmim]	$[NTf_2]$	298.15	81
	[HB]	293.15	105		[BETI]	298.15	218
	[Me-TCA]	323.15	34	$[C_2C_1im]$	$[NTf_2]$	298.15	69
	[CM-TCA]	323.15	95		[BETI]	298.15	186
	$[BF_4]$	298.15	41	[(1o1)mim]	$[CF_3BF_3]$	298.15	55
	$[CF_3BF_3]$	298.15	26		$[C_2F_5BF_3]$	298.15	47
	$[C_2F_5BF_3]$	298.15	27				
	$[C_3F_7BF_3]$	298.15	32	[(2o1)mim]	$[BF_4]$	298.15	200
	$[C_4F_9BF_3]$	298.15	38		$[CF_3BF_3]$	298.15	43
	[FSI]	298.15	18		$[C_2F_5BF_3]$	298.15	38
	$[NTf_2]$	298.15	37	$[C_6mim]$	$[BF_4]$	298.15	174
	[BETI]	298.15	61		$[CF_3BF_3]$	298.15	77
					$[C_2F_5BF_3]$	298.15	59
$[C_4mim]$	[TA]	293.15	73	[(2o2o1)mim]	$[BF_4]$	298.15	283
	[HB]	293.15	182				
					$[CF_3BF_3]$	298.15	62
	[TCA]	323.15	44		$[C_2F_5BF_3]$	298.15	51
	[Me-TCA]	323.15	52	$[C_3mim]$	$[BF_4]$	298.15	103
	[PCA]	323.15	65				
	[CM-TCA]	323.15	95		$[CF_3BF_3]$	298.15	43
					$[C_2F_5BF_3]$	298.15	35
	$[BF_4]$	298.15	112		$[C_3F_7BF_3]$	298.15	44
	$[CF_3BF_3]$	298.15	49		$[C_4F_9BF_3]$	298.15	59
	$[C_2F_5BF_3]$	298.15	41	$[BzC_2im]$	$[NTf_2]$	298.15	252
$[(2o1)C_1ox]$	$[BF_4]$	298.15	704		[BETI]	298.15	552
	$[CF_3BF_3]$	298.15	134	$[C_4C1ox]$	$[BF_4]$	298.15	731
	$[C_2F_5BF_3]$	298.15	90				
	$[C_3F_7BF_3]$	298.15	117		$[CF_3BF_3]$	298.15	165
	$[C_4F_9BF_3]$	298.15	177		$[C_2F_5BF_3]$	298.15	108
$[C_4C_1pyr]$	$[CF_3BF_3]$	298.15	137	$[C_1(1o1)pyr]$	$[BF_4]$	298.15	100
	$[C_2F_5BF_3]$	298.15	71		$[CF_3BF_3]$	298.15	46
	$[C_3F_7BF_3]$	298.15	62		$[C_2F_5BF_3]$	298.15	37
	$[C_4F_9BF_3]$	298.15	84	$[C_1(2o1)pyr]$	$[BF_4]$	298.15	213
	[FSI]	293.15	66		$[CF_3BF_3]$	298.15	87
	$[NTf_2]$	293.15	89		$[C_2F_5BF_3]$	298.15	52
[pyr]	[HCOO]	298.15	15	$[C_3C_1pyr]$	[FSI]	293.15	39
	[OAc]	298.15	30		$[NTf_2]$	293.15	61
	$[C_7H_{15}COO]$	298.15	37	$[C_3C_1pip]$	[FSI]	298.15	95
$[(2o1)C_1pip]$	$[BF_4]$	298.15	1240		$[NTf_2]$	298.15	151
	$[CF_3BF_3]$	298.15	203	$[C_4C_1mo]$	$[CF_3BF_3]$	298.15	1035
	$[C_2F_5BF_3]$	298.15	112				
	$[C_3F_7BF_3]$	298.15	131		$[C_2F_5BF_3]$	298.15	466
	$[C_4F_9BF_3]$	298.15	187	$[N_{HH},(C_2OH)_2]$	[HCOO]	298.15	762
$[(2o1)C_1mo]$	$[CF_3BF_3]$	298.15	471		[OAc]	298.15	5647
	$[C_2F_5BF_3]$	298.15	260	$[N_{HHH},C_2OH]$	[HCOO]	298.15	105
	$[C_3F_7BF_3]$	298.15	777		[OAc]	298.15	701
$[N_{1HH},C_2OH]$	[HCOO]	298.35	20.27	$[N_{23'3'H}]$	[HCOO]	298.15	18
	[OAc]	298.15	106.06				
	$[C_2COO]$	298.20	215.06		[OAc]	298.15	54
	$[C_3COO]$	298.15	298.15	$[N_{13'3'H}]$	[HCOO]	298.15	25
$[N_{2HHH}]$	[HCOO]	298.15	32		[OAc]	298.15	32
	$[C_2COO]$	298.15	75	[EDA]	[HCOO]	298.15	112
	$[C_3COO]$	298.15	208		[OAc]	298.15	958

QSPR Results. The obtained two correlation equations for $[DCA]^-$- and $[P_{444},C_3NH_2]^+$-based ILs are presented in Table 7, where the equation verification results from testing data are also given. As indicated from the values of R^2 and S^2 (Table 7), testing data validation (Table 7) and inner validation (Figure 7), the QSPR equations are reliable.

Set A ($[DCA]^-$, 298 K). As shown in Eq. 1 (Table 7), there are one topological descriptor (D_1), one electrostatic descriptor (D_4), and two quantum chemical descriptors (D_2, D_3). The values of t-test indicate that the importance of descriptors decrease in the following order: $D_1 > D_2 > D_4 > D_3$.

D_1, Randic index (order 2), which has the most important effect on the viscosity, is defined as $R(\Gamma) = \sum_{v_i \sim v_j} \frac{1}{\sqrt{\delta_i \delta_j}}$,

Table 5. Viscosity Comparison Between Column A and Column B to Understand the Effects on ILs Viscosity of F Atom on Anion (in cP at 298 K)

Column A		Column B	
ILs	Viscosity	ILs	Viscosity
$[C_2mim][CH_3BF_3]$	47	$[C_2mim][CF_3BF_3]$	26
$[C_2mim][C_2H_5BF_3]$	72	$[C_2mim][C_2F_5BF_3]$	27
$[C_2mim][C_3H_7BF_3]$	54	$[C_2mim][C_3F_7BF_3]$	32
$[C_2mim][C_4H_9BF_3]$	83	$[C_2mim][C_4F_9BF_3]$	38
$[C_4mim][C_5F_5SO_4]$	250	$[C_4mim][C_5F_8SO_4]$	170
$[C_4C_1mim][C_5F_5SO_4]$	3200	$[C_4C_1mim][C_5F_8SO_4]$	840
$[C_2mim][TA]$	35*	$[C_2mim][OAc]$	162*
$[C_4mim][TA]$	73*	$[C_4mim][OAc]$	646*
[Pyr][TA]	21	[Pyr][OAc]	30

*At 293 K.

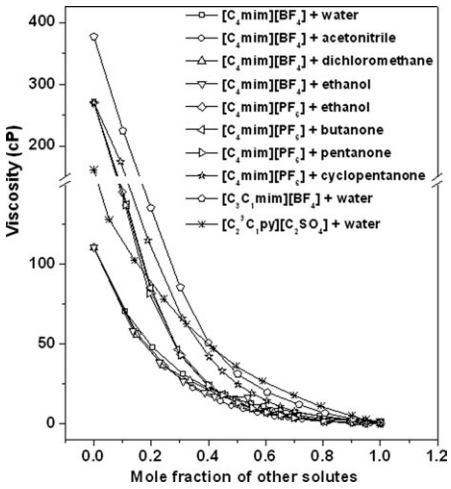

Figure 5. The effects of other solutes on the viscosity of ILs (at 298 K).

Table 6. Selected Viscosity Data for the QSPR Study (at 1 atm, in cP)*

Set	Abbreviation	Viscosity (η)	Log η
A	*[C2mim][DCA]*	*21*	*1.322*
	[C4mim][DCA]	28.8	1.459
	[C6mim][DCA]	47.4	1.675
	[C8mim][DCA]	34	1.531
	[C10mim][DCA]	76	1.88
	[C4C1mim][DCA]	67.2	1.827
	[Bzmim][DCA]	40	1.602
	[(Bz)2im][DCA]	202	2.305
	[C4 3C1py][DCA]	36.26	1.559
	[C2C1pyr][DCA]	27.5	1.439
	[C3C1pyr][DCA]	45	1.653
	[C4C1pyr][DCA]	36.5	1.562
	[C6C1pyr][DCA]	45	1.653
	[S111][DCA]	27.2	1.435
	[S133][DCA]	29.5	1.470
	[S112][DCA]	25.3	1.403
	[S222][DCA]	*20.9*	*1.320*
	[S244][DCA]	51.7	1.713
	[S144][DCA]	60	1.778
	[S233][DCA]	29.4	1.468
	[N1888][DCA]	300	2.477
	[C2C1pyra][DCA]	24.6	1.391
	[(C6C6)2(C1)2gua][DCA]	267	2.427
B	[P444,C3NH2][Ala]	54.3	1.735
	[P444,C3NH2][Arg]	124.8	2.096
	[P444,C3NH2][Asn]	*447.1*	*2.651*
	[P444,C3NH2][Asp]	481.8	2.683
	[P444,C3NH2][Cys]	775.5	2.890
	[P444,C3NH2][Gln]	377.7	2.577
	[P444,C3NH2][Glu]	434.9	2.638
	[P444,C3NH2][Gly]	54.2	1.734
	[P444,C3NH2][His]	313.7	2.497
	[P444,C3NH2][Ile]	73.8	1.868
	[P444,C3NH2][Leu]	66.2	1.821
	[P444,C3NH2][Lys]	81.7	1.912
	[P444,C3NH2][Met]	55.9	1.747
	[P444,C3NH2][Phe]	88.2	1.945
	[P444,C3NH2][Pro]	81.8	1.913
	[P444,C3NH2][Ser]	*71.6*	*1.855*
	[P444,C3NH2][Thr]	84.5	1.927
	[P444,C3NH2][Val]	56.3	1.751
	[P444,C3NH2][Tyr]	1291.0	3.111

where δ_i denotes the degree of the vertex v_i.[85] The descriptor encodes the size, shape, and degree of branching in the cations and also relates to the dispersion interaction among ions.[86] D_2, HACA H-acceptors charged surface area [quantum-chemical PC], is defined as HACA-1 = ΣS_A, $A \in H_{\text{H-acceptor}}$, where s_A is solvent-accessible surface area of H-bonding acceptor atoms selected by threshold charge,[87] and this descriptor indicates the effect of hydrogen-bonding ability of cation on the viscosity.[88] D_4, polarity parameter/square distance, is calculated as the difference between the maximum and the minimum charges factorized by the square of the distance between the atoms that bear minimum and maximum partial charges.[89] This descriptor characterizes the polarity of cation.[90] D_3, average 1-electron reactive index for a C atom, relates to the strength of intramolecular bonding interactions, characterizes the stability of the molecules, and reflects the electrostatic and hydrogen bonding interactions among ions.[91]

Set B ($[P_{444},C_3NH_2]^+$, 384.15 K). As shown in Eq. 2 (Table 7), the importance of descriptors decreases in the following order: $D_5 > D_7 > D_8 > D_6$, and D_8 is thermodynamic descriptor while the others are quantum-chemical descriptors.

D_5, average 1-electron reactive index for a O atom, is closely related with the forming of the hydrogen bonding because of the isolated electrons of O atom and has the most important effect on the viscosity.[92] D_7, DPSA-1 difference in charge partial surface areas (CPSAs) (PPSA1–PNSA1) [quantum-chemical PC] (here, CPSA is a class of descriptors), is defined as DPSA-1=PPSA-1 − PNSA-1, where PPSA-1 is positively charged solvent-accessible molecular surface area and PNSA-1 is negatively charged solvent-accessible molecular surface area, and describes the difference in the positive and negative charges of the partial surface area.[87] The larger value of the descriptor indicates a higher polarity of the anion. The negative regression coefficient for this descriptor reflects the fact that the larger value of this descriptor leads to lower binding ability.[93] D_6, Tot hybridization component of the molecular dipole, encodes the size and polarity of the anion, and is directly related to electrostatic dipole–dipole interactions in condensed phase.[94] D_8, complementary information content (order 2), is defined as

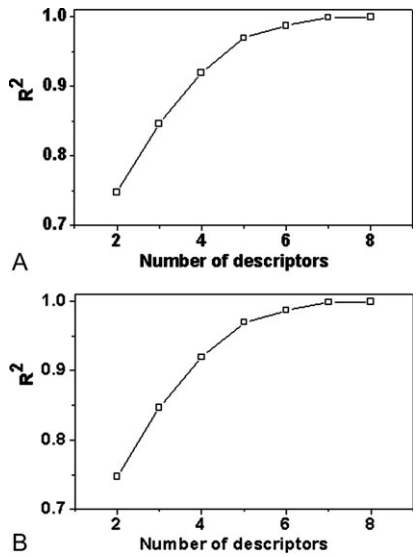

Figure 6. R^2 vs. descriptor number for set A and set B.

Table 7. Four-Parameter Correlation Equations of Viscosity for $[DCA]^-$-Based and $[P_{444},C_3NH_2]^+$-Based ILs, Along with Equation Verification

	Equation						Equation Verification				
No.	Descriptor No.	Descriptor Symbol	X*	ΔX†	t-test‡	Characteristic Parameter§	IL	Exp. $\log \eta$	Cal. $\log \eta$	Absolute Deviation	Relative Deviation (%)
Equation 1 (Set A)	0	Intercept	1.1541	$4.0997E-2$	28.15		$[C_2mim][DCA]$	1.2670	1.3378	0.0708	5.59
	1	D_1	$1.6957E-1$	$1.1377E-2$	14.91	$R^2 = 0.9578$					
	2	D_2**	$-2.7118E-1$	$5.3187E-2$	−5.10	$R^2_{CV} = 0.9353$	$[(C_6C_6)_2(C_1)_2gua][DCA]$	1.3743	0.0543	4.11	1.37
	3	D_3**	$-1.0713E2$	3.7337*E*1	−2.87	$F = 96.44$					
	4	D_4††	−7.4486	1.8157	−4.10	$s^2 = 0.0055$					
Equation 2 (Set B)	0	Intercept	2.8569	$5.5156E-2$	51.80		$[P_{444},C_3NH_2][Asn]$	3.2130	3.4435	0.2305	7.17
	1	D_5**	$-1.1862E2$	1.4274*E*1	−8.31	$R^2 = 0.9196$					
	2	D_6**	$-8.1707E-2$	$2.4324E-2$	−3.36	$R^2_{CV} = 0.9113$	$[P_{444},C_3NH_2][Ser]$	3.0390	3.2166	0.1776	5.84
	3	D_7**	$-1.3836E-3$	$2.5787E-4$	−5.37	$F = 28.61$					
	4	D_8‡‡	$1.0475E-2$	$2.6140E-3$	4.01	$s^2 = 0.8402$					

*Regression coefficient of the linear model.
†Standard error for each regression coefficient.
‡t-test values for each coefficient.
§In the correlation, R^2 is correlation coefficient, F is Fisher significance parameter, R^2_{CV} is cross-validated correlation coefficient, and s^2 is corrected mean square error.
¶Topological descriptor for describing the atomic connectivity in the molecule.
**Quantum chemical descriptor.
††Electrostatic descriptor.
‡‡Thermodynamic descriptor.

${}^kCIC = \log_2 n - {}^kIC$, ${}^kIC = -\sum_{i=1}^{k} \frac{n_i}{n} \log_2 \frac{n_i}{n}$, where n_i is number of atoms in the ith class, n is the total number of atoms in the molecule, and k is number of atomic layers in the coordination sphere around a given atom that are accounted for.[95] This descriptor encodes the molecular geometric characteristic.

QSPR Summary. The previous QSPR results for ILs viscosity, coupled with the results in this study, are summarized in Table 8. As indicated in Table 8, the cation–anion electrostatic, hydrogen bonding and van der Waals interaction give important effects on ILs viscosity, and other factors such as polarizability and ionic geometric characteristic (shape, branching degree, and symmetry) also give some effects, which is somewhat different from molecular-type compounds where the main factors are hydrogen bonding and van der Waals interaction.[96–98] Such interactions deduced from QSPR quantitative correlations on ILs viscosity are consistent with the aforementioned analysis from direct observation. Let us take interionic hydrogen bonding interaction as example. As indicated in Table 3, the atoms or groups such as —OH, —SR, —COOH, —C≡N, and —F on cation will increase the viscosity, e.g., $[CH_3CH(OH)CH_2mim][NTf_2]$ (342 cP at 298 K) vs. $[C_4mim][NTf_2]$ (45 cP at 298 K), $[C_3COOHmim][CH_3CH(BF_3)CH_2CN]$ (3047 cP at 273 K) vs. $[C_4mim][CH_3CH(BF_3)CH_2CN]$ (101 cP at 273 K); as indicated in Supporting Information Table S11, sharing a common cation, the viscosity for $[OAc]^-$ is the highest in the order of $[DCA]^- < [NTf_2]^- < [TfO]^- < [BF_4]^- < [PF_6]^- < [OAc]^-$; such hydrogen bonding interaction observed directly is found in the QSPR study of Set $[DCA]^-$ (indicated by D_2 and D_3) and Set $[P_{444},C_3NH_2]^+$ (D_5) in this work, Set $[BF_4]^-$ (D_2) and Set $[NTf_2]^-$ (D_7) of Han et al.,[32] and Set $[NTf_2]^-$ (D_{13} and D_{14}) of Yu et al.[33] As indicated in Table 8, the effects of interionic hydrogen bonding and van der Waals interaction on the viscosity for $[P_{444},C_3NH_2]^+$-based ILs with positive-charge-center and bulky alkyl side chains and the $[DCA]^-$-based ILs with much disperse charge

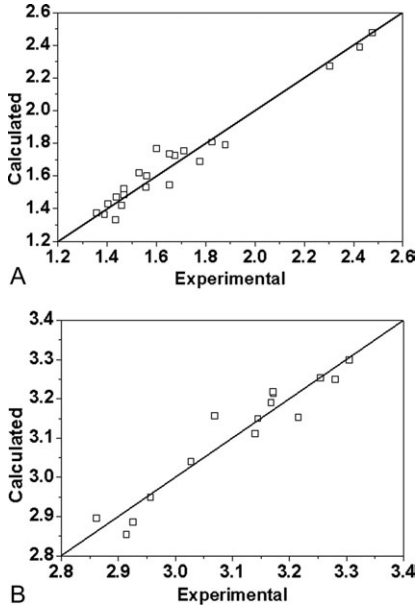

Figure 7. Scatter plots of the calculated vs. experimental values of viscosity (in 10^{-3} Pa s) for the ILs in training data.

Table 8. Results of QSPR Study on the Viscosity of ILs

No.	Results	References
1	System: 32 ILs at 293 K; cation: imidazolium, pyridium, piperidinium, and morpholinium; anion: bis(trifluoromethylsulphonyl) imide. Method: Heuristic method. Equation: η (cP) $= -71.852 - 14507\ D_1 + 10005\ D_2 + 291.55\ D_3 - 0.3731\ D_4$ ($R^2 = 0.8755$, $R^2_{CV} = 0.7647$, $F = 42.18$). Descriptor: D_1, FNSA-3 fractional PNSA, is a measurement of the negatively charged surface area accessible to the surrounding molecules; D_2, maximum 1-electron reactive index for a C atom, is a Fukui function designed specifically to describe chemical reactions; D_3, polarity parameter ($Q_{max} - Q_{min}$), is defined as $P = Q_{max} - Q_{min}$, Q_{max} is the most positive atomic partial charge in the molecule, Q_{min} is the most negative atomic partial charge in the molecule; D_4, highest normal mode vib. frequency. Observation: D_1 and D_2 has the most important effect on the viscosity, which indicate the cation–anion electrostatic or donor–acceptor interactions; D_3 characterizes the polarity of cation; although R^2 (0.8755) for the equation is satisfying, the correlation is not capable of matching well two regions of low (nonmorpholinium) and high (morpholinium) viscosity at the same time.	22
2	System: 17 ILs at 298.15 K; cation: imidazolium; anion: tetrafluoroborate ($[BF_4]^-$). Method: BMLR Equation: η (cP) $= -439.88 - 1.1555\ D_1 - 17518\ D_2 + 602.35\ D_3 + 3596.6\ D_4$ ($R^2 = 0.9374$, $R^2_{CV} = 0.8671$, $F = 33.70$, $s^2 = 902.21$). Descriptor: D_1, PNSA2 total charge weighted PNSA, is defined as PNSA2 $= \sum q_A \sum S_A$, $A \in \{\Delta_A < 0\}$, S_A is negatively charged solvent-accessible atomic surface area, q_A is atomic partial charge; D_2, HACA2/TMSA, is defined as HACA2/TMSA $= \sum(q_A S_A^{1/2}/S_{tot}^{1/2})$/TMSA, $A \in X_{H\text{-acceptor}}$, S_A is solvent-accessible surface area of H-bonding acceptor atoms, selected by threshold charge, q_A is partial charge on H-bonding acceptor atoms, selected by threshold charge, S_{tot} is total solvent-accessible molecular surface area; D_3, Min net atomic charge for a C atom, which is minimum net atomic charge for a C atom; D_4, FPSA3 fractional PPSA, is defined as FPSA3 = PPSA3/TMSA**,** PPSA3 is total charge weighted partial positively charged molecular surface, TMSA is total molecular surface area; Observation: D_1 is total charge weighted partial negative surface area; D_4 is fractional atomic charge on a partial positively charged surface area; thus, a larger accessible surface area with a negative partial charge and a less accessible surface area with a positive partial charge will lower viscosity, the above two descriptors indicate the charge property of molecule and further partially account for the cation–anion electrostatic interaction in the ILs; D_2 indicates the effect of hydrogen-bonding ability of cation on the viscosity; D_3 partially represents the effect of cation–anion electrostatic interaction or cation dipole moment on the viscosity.	32
3	System: 18 ILs at 298.15 K; cation: imidazolium; anion: bis(trifluoromethylsulfonyl)imide ($[NTf_2]^-$). Method: BMLR Equation: η (cP) $= 154.29 - 5421.3\ D_5 + 0.00000482\ D_6 + 1125.8\ D_7 + 0.64155\ D_8$ ($R^2 = 0.9692$, $R^2_{CV} = 0.9113$, $F = 78.58$, $s^2 = 36.19$). Descriptor: D_5, Min electrophilic reactive index for a N atom, is defined as EA $= \sum c^2_{jLUMO}/\varepsilon_{LUMO} + 10)$, c_{jLUMO} is the lowest unoccupied molecular orbital energy; c_{jLUMO} is the lowest unoccupied molecular orbital MO coefficients; D_6, vib. enthalpy (300 K)/no. of atoms, is defined as $H_{vib} = 0.5\sum h\nu_i + h\nu_i \exp(-h\nu_i/2kT)/[1 - \exp(-h\nu_i/2kT)]$, n_j is frequencies of normal vibrations in the molecule; h is Planck's constant; k is Boltzmann's constant; T is absolute temperature (K); D_7, HA dependent HDCA1/TMSA, is defined as HDCA1/TMSA $= \sum(S_D$/TMSA), $D \in H_{H\text{-donor}}$, S_D is solvent-accessible surface area of hydrogen-bonding donor H atoms, selected by threshold charge; D_8, 1X BETA polarizability (DIP), is defined as $\mu' = \mu + \alpha E + 0.5\beta E^2 + \ldots$, μ is permanent dipole moment of the molecule; μ' is induced dipole moment of the molecule, E is external electric field; Observation: D_7 indicates that the hydrogen-bonding donor ability of cation; the larger is the hydrogen-bonding donor ability of cation, the higher is the viscosity; D_5 has the most important effect, and gives a measure of the reactivity of cation, i.e., the nucleophilicity of N atom. A low value of this descriptor will lead to an increase in viscosity; D_6 reflects the effect of atom vibration of cation on the viscosity; D_8 partially represents the effect of van der Waals interaction between cation and anion on the viscosity.	32
4	System: 17 ILs at 298.15 K; cation: 1-butyl-3-methylimidazolium ($[C_4mim]^+$). Method: BMLR Equation: η (cP) $= 192.4 - 101.85\ D_9 + 3530{,}000\ D_{10} + 155.79\ D_{11} + 20.618\ D_{12}$ ($R^2 = 0.9220$, $R^2_{CV} = 0.7679$, $F = 29.54$, $s^2 = 1719.71$). Descriptor: D_{10}, Min atomic orbital electronic population, is atomic orbital electronic population for a given atomic species in the molecule; D_9, No. of occupied electronic levels/no. of atoms, is related to molecular polarizability; D_{11}, moment of inertia C, is calculated as follows: Ik $= \sum m_i r_{ik}^2$, m_i is atomic weights of constituent atoms of a molecule, r_{ik} is distance of the ith atomic nucleus from the kth main rotational axes ($k = X$, Y, or Z); D_{12}, structural information content (order 1), is defined on Shannon information theory as, $^kSIC = {}^kIC/\log_2 n$, and $^kIC = -\sum(n_i/n)\log_2(n_i/n)$, n_i is number of atoms in the ith class; n is the total number of atoms in the molecule; k is number of atomic layers in the coordination sphere around a given atom that are accounted for; Observation: The most important descriptor of this model is D_{10}, which is a simplified index to describe the nucleophilicity ability of the molecule and represents the quantum-chemically calculated charge distribution in the molecules, and therefore describes, in a very accurate way, the polar interactions between molecules or their cation–anion electrostatic interaction; D_9 is related to molecular polarizability because the higher the number of the electronic shells, the more polarizable the molecule, and it also partially reflects the polar interactions between cation and anion; D_{11} shows that the greater the rotational inertia of anions, the greater the viscosity, and that the volume and quality of the moment inertia on anions are closely related. Therefore, it is expected that the smaller the molecular volume, the smaller the viscosity of the ILs; D_{12} describes the connectivity and branching in a molecule, therefore, the viscosity is related to anionic shape and symmetry; the polar interactions between molecules or their cation–anion electrostatic interaction have the most important effect on the viscosity; the polar interactions between cation and anion give less impact on viscosity; the rotational inertia of anions and anionic shape and symmetry give some contributions.	32

Table 8. (Continued)

No.	Results	References
5	System: 24 ILs at 298.15 K; cation: 1-ethyl-3-methylimidazolium ($[C_2mim]^+$). Method: BMLR Equation: η (cP) $= -54.388 + 95.164\ D_{13} + 64.34\ D_{14} + 19.294\ D_{15} - 4.0687\ D_{16}$ ($R^2 = 0.9327$, $R^2_{CV} = 0.9004$, $F = 55.47$, $s^2 = 46.53$). Descriptor: D_{14}, RPCG Relative positive charge (QMPOS/QTPLUS), is defined as: RPCG $= \Delta_{max}/\Delta A$, $A \in \{\Delta_A > 0\}$, Δ_{max} is maximum atomic positive charge in the molecule; Δ_A is positive atomic charge in the molecule; D_{13}, FPSA2 fractional PPSA, is defined as FPSA2 = PPSA2/TMSA, PPSA2 is total charge weighted partial positively charged molecular surface area; D_{15}, the Randic index (order 0), is a measure of the compactness of the molecule; D_{16}, translational heat capacity (300 K)/no. of atoms, is translational heat capacity (300 K) of atoms; Observation: The most important descriptor, D_{14}, is an anion descriptor which increases with highly localized positive charge; the positive coefficient for D_{14} indicates that localization of positive charge on anions will reduce the viscosity. Therefore, monatomic anion such as chloride is predicted to be higher viscosity than very large anions containing regions of positive charge such as bis(trifluoromethanesulfonyl)imide, as is consistent with their experimental values of viscosity; D_{13} is partially accounts for the electrostatic interaction between cation and anion; D_{15} has a topological origin and is a measure of the compactness of the molecule, and indicates that the magnitude of cation–anion interaction is related to the degree of branching of anion as well as to anion size, so, D_{12} and D_{15} reflect the effect of anion structural complex on viscosity; the most important D_{11} reflects the electrostatic or charge transfer interaction between cation and anion; the spatial shape of cation (including branching and symmetry) and the hydrogen bonding interaction between cation and anion have important effects on the viscosity.	32
6	System: 106 ILs at 298 K; anion: bis(trifluoromethylsulfonyl)imide ($[NTf_2]^-$). Cation: imidazolium, pyridinium, pyrrolidinium, sulfonium, ammonium, morpholinium, phosphonium, oxazolidinium, guanidinium, and piperidinium. Method: BMLR Equation: log η (cP) $= -0.8531 + 0.04418\ D_{10} + 3.5232\ D_{11} + 0.1771\ D_{12} + 0.2147\ D_{13} - 10.567\ D_{14} + 0.5445\ D_{15} - 0.1035\ D_{16}$ ($R^2 = 0.8226$, $R^2_{CV} = 0.7236$, $F = 41.73$, $s^2 = 0.033$). Descriptor: D_{11}, FNSA-1 fractional PNSA (PNSA-1/TMSA), is defined as FNSA-1 = PNSA-1/TMSA, PNSA-1 is partial negatively charged molecular surface area; D_{10}, bonding information content (order 2), gives the information about the spatial shape of cation; D_{13}, HACA-1, is defined as HACA-1 $= \sum S_A$, $A \in H_{H\text{-acceptor}}$, s_A is solvent-accessible surface area of H-bonding acceptor atoms, selected by threshold charge; D_{12}, LUMO+1 energy, reflects the electrophilic ability of cation and the donor–acceptor interaction with the anion; D_{14}, Max partial charge for an H atom, is the Max partial charge for a H atom; D_{15}, number of benzene rings, denotes the number of benzene ring; D_{16}, relative positive charged SA (SAM-POS*RPCG), is defined as the most positive surface area in a molecule, characterizing the charge redistribution; Observation: D_{11} reflects the electrostatic or charge transfer interaction between cation and anion; D_{10} gives the information about the spatial shape of cation (including branching and symmetry), the positive coefficient indicates the larger the value of the descriptor the higher the viscosity; D_{13} reflects hydrogen bonding acceptor ability of cation and the hydrogen bonding interaction between cation and anion; D_{12} reflects the electrophilic ability of cation and the donor–acceptor interaction with the anion; D_{14} is the Max partial charge for a H atom; D_{15} indicates that the more benzene ring, the higher the viscosity; D_{16} encodes the molecular electrostatic and hydrogen-bonding ability features; the electrostatic or charge transfer interaction between cation and anion has the most important effect on the viscosity, the shape of cation (including branching and symmetry) has the second most important effect; hydrogen-bonding ability also has an important effect on the viscosity.	33
7	System: 23 ILs at 298.15 K; anion: dicyanamide ($[DCA]^-$). Cation: imidazolium, pyridinium, pyrrolidinium, sulfonium, ammonium, guanidinium, and pyrazolium. Method: BMLR Equation: log η (cP) $= 1.1541 + 0.1696\ D_1 - 0.2712\ D_2 - 107.13\ D_3 - 7.4486\ D_4$ ($R^2 = 0.9578$, $R^2_{CV} = 0.9353$, $F = 96.44$, $s^2 = 0.0055$). Descriptor: D_1, the Randic index (order 2), is defined as $R(\Gamma) = \sum(\delta i \delta_j)^{-0.5}$, where Δ_i denotes the degree of the vertex v_i. D_2, HACA H-acceptors charged surface area [quantum-chemical PC], is defined as HACA-1 $= \sum S_A$, $A \in H_{H\text{-acceptor}}$, s_A is solvent-accessible surface area of H-bonding acceptor atoms, selected by threshold charge. D_4, polarity parameter/square distance, is calculated as the difference between the maximum and the minimum charges factorized by the square of the distance between the atoms that bear minimum and maximum partial charges; D_3, average 1-electron reaction index for a C atom, relates to the strength of intramolecular bonding interactions and characterizes the stability of the molecules. Observation: D_1 encodes the size, shape, and degree of branching in the cations and also relates to the dispersion interaction among ions; D_2 indicates the effect of hydrogen-bonding ability of cation on the viscosity; D_4 characterizes the polarity of cation; D_3 characterizes the stability of the molecules, and reflects the electrostatic and hydrogen bonding interactions among ions; the size, shape, and degree of branching in the compound and also relates to the dispersion interaction among molecules, has the most important effect on the viscosity; hydrogen-bonding ability of cation and polarity of the molecule also have important effects on the viscosity.	This work
8	System: 19 ILs at 298.15 K; cation: tributyl-(3-amino-propyl) phosphonium ($[P_{444},C_3NH_2]^+$). Method: BMLR Equation: log η (cP) $= 2.8569 - 118.62\ D_5 - 0.08171\ D_6 - 0.001384\ D_7 + 0.01048\ D_8$ ($R^2 = 0.9196$, $R^2_{CV} = 0.9113$, $F = 28.61$, $s^2 = 0.8402$). Descriptor: D_5, average 1-electron reactive index for a O atom, is closely related with the forming of the hydrogen bonding because of the isolated electrons of O atom; D_7, DPSA-1 difference in CPSAs (PPSA1-PNSA1) [quantum-chemical PC], is defined as DPSA-1 = PPSA-1–PNSA-1, where PPSA-1 is positively charged solvent-accessible molecular surface area and PNSA-1 is negatively charged solvent-accessible molecular surface area; D_6, Tot hybridization comp. of the molecular dipole, characterizes the size and polarity of the molecule; D_8, complementary information content (order 2), is defined as, ${}^kCIC = \log_2 n - {}^kIC$, ${}^kIC = -\sum(n_i/n)\log_2(n_i/n)$, where n_i is number of atoms in the ith class, n is the total number of atoms in the molecule, and k is number of atomic layers in the coordination sphere around a given atom that are accounted for. Observation: D_5 is closely related with the forming of the hydrogen bonding because of the isolated electrons of O atom; D_7 describes the difference in the positive and negative of the partial surface area. The larger value of the descriptor indicates the higher polarity of the anion. The negative regression coefficient for this descriptor reflects the fact that the larger value of this descriptor leads to lower binding ability; D_6, Tot hybridization comp. of the molecular dipole, encodes the size and polarity of the anion, and is directly related to electrostatic dipole–dipole interactions in condensed phase; D_8 encodes the molecular geometric characteristic; the hydrogen bonding has the most important effect on the viscosity; the size and polarity of the molecule also have important effects on the viscosity.	This work

distribution, are more remarkable than that for other $[C_4mim]^+$-, $[C_2mim]^+$-, $[NTf_2]^-$-, and $[BF_4]^-$-based ILs.

Conclusions

Viscosity is a vital physical property for ILs. In this work, a database for the viscosity of pure ILs and their binary/ternary mixtures with molecular compounds is established by performing a comprehensive collection covering the period from 1970 to 2009, in which a variety of necessary information such as the basic information (name, ID, abbreviation, formula, molecular weight, structural formula, and CAS number), sample information (sample sources, initial and final purity, purification method, and purity analysis), and viscosity information (temperature, pressure, viscosity value, measurement methods or model, and reference) are included, and 5046 data entries, 696 ILs, 306 cations, and 138 anions are finally used. Following the database, a direct observation of the effects of ionic structure (e.g., length of alkyl side chain on cation, type of cation ring, characteristic atom/group on cation, anion type, anion size, and fluoronation of the alkyl chain in anion) along with temperature, pressure, and impurity on the viscosity is summarized, and a QSPR correlation is performed for two selected $[DCA]^-$- and $[P_{444},C_3NH_2]^+$-based ILs. Besides temperature, pressure, and impurity, the ionic structural characteristics of cation or anion of ILs has significant effects on the viscosity; the cation–anion electrostatic interaction determined by ionic structural characteristics gives the most effect on viscosity, followed by interionic hydrogen bonding and van der Waals interaction, which is different from traditional molecular-type organic solvents. To this end, the structure of cation and anion of ILs, as well as the interionic interaction (especially electrostatic, interionic hydrogen bonding, and van der Waals), should be carefully tailored for obtaining an IL with desired viscosity.

Acknowledgments

This work was financially supported by the National Natural Science Foundation of China (20806002, 20976005, and 21176021), the Beijing Natural Science Foundation (2103051), and the Petro China Innovation Foundation (2010D-5006-0403).

Literature Cited

1. Brennecke JF, Maginn EJ. Ionic liquids: innovative fluids for chemical processing. *AIChE J*. 2001;47:2384–2389.
2. Earle MJ, Esperanca JMSS, Gilea1 MA, Lopes JNC, Rebelo LPN, Magee JW, Seddon KR, Widegren JA. The distillation and volatility of ionic liquids. *Nature*. 2006;439:831–834.
3. Zaitsau DH, Kabo GJ, Strechan AA, Paulechka YU, Tschersich A, Verevkin SP, Heintz A. Experimental vapor pressures of 1-alkyl-3-methylimidazolium bis(trifluoromethylsulfonyl)imides and a correlation scheme for estimation of vaporization enthalpies of ionic liquids. *J Phys Chem A*. 2006;110:7303–7306.
4. Santos LMNBF, Lopes CJN, Coutinho JAP, Esperanca JMSS, Gomes LR, Marrucho IM, Rebelo LPN. Ionic liquids: first direct determination of their cohesive energy. *J Am Chem Soc*. 2007;129:284–285.
5. Blanchard LA, Hancu D, Beckman EJ, Brennecke JF. Ionic liquid/CO_2 biphasic systems: new media for green processing. *Nature*. 1999;399:28–29.
6. Huddleston JG, Visser AE, Reichert WM, Willauer HD, Broker GA, Rogers RD. Characterization and comparison of hydrophilic and hydrophobic room temperature ionic liquids incorporating the imidazolium cation. *Green Chem*. 2001;3:156–164.
7. Zhang SJ, Sun N, He XZ, Lu XM, Zhang XP. Physical properties of ionic liquids: database and evaluation. *J Phys Chem Ref Data*. 2006;35:1475–1517.
8. Anthony JL, Anderson JL, Maginn EJ, Brennecke JF. Anion effects on gas solubility in ionic liquids. *J Phys Chem B*. 2005;109:6366–6374.
9. Liu JH, Cheng SQ, Zhang JL, Feng XY, Fu XG, Han BX. Reverse micelles in carbon dioxide with ionic liquid domains. *Angew Chem Int Ed Engl*. 2007;46:3313–3315.
10. Widegren JA, Magee JW. Density, viscosity, speed of sound, and electrolytic conductivity for the ionic liquid 1-hexyl-3-methylimidazolium bis(trifluoromethylsulfonyl)imide and its mixtures with water. *J Chem Eng Data*. 2007;52:2331–2338.
11. Burrell GL, Burgar IM, Separovicc F, Dunlop NF. Preparation of protic ionic liquids with minimal water content and 15N NMR study of proton transfer. *Phys Chem Chem Phys*. 2010;12:1571–1577.
12. Anderson JL, Armstrong DW. High-stability ionic liquids. a new class of stationary phases for gas chromatography. *Anal Chem*. 2003;75:4851–4858.
13. Mu Z, Liu W, Zhang S, Zhou F. Functional room-temperature ionic liquids as lubricants for an aluminum-on-steel system. *Chem Lett*. 2004;33:524–525.
14. Katritzky AR, Lomaka A, Petrukhin R, Jain R, Karelson M, Visser AE, Rogers RD. QSPR correlation of the melting point for pyridinium bromides, potential ionic liquids. *J Chem Inf Comput Sci*. 2002;42:71–74.
15. Trohalaki S, Pachter R. Prediction of melting points for ionic liquids. *QSAR Comb Sci*. 2005;24:485–490.
16. Varnek A, Kireeva N, Tetko IV, Baskin II, Solov'ev VP. Exhaustive QSPR studies of a large diverse set of ionic liquids: how accurately can we predict melting points? *J Chem Inf Model*. 2007;47:1111–1122.
17. López-Martin I, Burello E, Davey PN, Seddon KR, Rothenberg G. Anion and cation effects on imidazolium salt melting points: a descriptor modeling study. *ChemPhysChem*. 2007;8:690–695.
18. Carrera GVSM, Branco LC, Aires-de-Sousa J, Afonso CAM. Exploration of quantitative structure-property relationships (QSPR) for the design of new guanidinium ionic liquids. *Tetrahedron*. 2008;64:2216–2224.
19. Eike DM, Brennecke JF, Maginn EJ. Predicting melting points of quaternary ammonium ionic liquids. *Green Chem*. 2003;5:323–328.
20. Trohalaki S, Pachter R, Drake GW, Hawkins T. Quantitative structure-property relationships for melting points and densities of ionic liquids. *Energy Fuels*. 2005;19:279–284.
21. Matsuda H, Yamamoto H, Kurihara K. Computer-aided reverse design for ionic liquids by QSPR using descriptors of group contribution type for ionic conductivities. *Fluid Phase Equilib*. 2007;261:434–443.
22. Bini R, Malvaldi M, Pitner WR, Chiappe C. QSPR correlation for conductivities and viscosities of low-temperature melting ionic liquids. *J Phys Org Chem*. 2008;21:622–629.
23. Lazzús JA. ρ(T, p) model for ionic liquids based on quantitative structure-property relationship calculations. *J Phys Org Chem*. 2009;22:1193–1197.
24. Couling DJ, Bernot RJ, Docherty KM, Dixona JK, Maginn EJ. Assessing the factors responsible for ionic liquid toxicity to aquatic organisms via quantitative structure–property relationship modeling. *Green Chem*. 2006;8:82–90.
25. Luis P, Ortiz I, Aldaco R, Irabien A. A novel group contribution method in the development of a QSAR for predicting the toxicity (Vibrio fischeri EC50) of ionic liquids. *Ecotoxicol Environ Saf*. 2007;67:423–429.
26. Gardas RL, Coutinho JAP. Applying a QSPR correlation to the prediction of surface tensions of ionic liquids. *Fluid Phase Equilib*. 2008;265:57–65.
27. Ge ML, Li CQ, Ma J. QSPR analysis for infinite dilution activity coefficients of organic solutes in ionic liquids. *Electrochemistry*. 2009;77:745–747.
28. Gardas RL, Coutinho JAP. Applying a QSPR correlation to the prediction of surface tensions of ionic liquids. *Fluid Phase Equilibria*. 2008;265:57–65.
29. Tamm K, Burk P. QSPR analysis for infinite dilution activity coefficients of organic compounds. *J Mol Model*. 2006;12:417–421.
30. Eike DM, Brennecke JF, Maginn EJ. Predicting infinite-dilution activity coefficients of organic solutes in ionic liquids. *Ind Eng Chem Res*. 2004;43:1039–1048.
31. Tochigi K, Yamamoto H. Estimation of ionic conductivity and viscosity of ionic liquids using a QSPR model. *J Phys Chem C*. 2007;111:15989–15994.
32. Han C, Yu GR, Wen L, Zhao DC, Chen XC. Data and QSPR study for viscosity of imidazolium-based ionic liquids. *Fluid Phase Equilib*. 2010;300:93–102.

33. Yu GR, Wen L, Zhao DC, Chen XC. QSPR study on the viscosity of bis(trifluoromethylsulfonyl)imide-based ionic liquids. *J Phys Chem B*. In press.
34. Dzyuba SV, Bartsch RA. Influence of structural variations in 1-alkyl(aralkyl)-3-methylimidazolium hexafluorophosphates and bis(trifluoromethylsulfonyl) imides on physical properties of the ionic liquids. *ChemPhysChem*. 2002;3:161–166.
35. Seki S, Kobayashi T, Kobayashi Y, Takei K, Miyashiro H, Hayamizu K, Tsuzuki S, Mitsugi T, Umebayashi Y. Effects of cation and anion on physical properties of room-temperature ionic liquids. *J Mol Liq*. 2010;152:9–13.
36. Zhou ZB, Matsumoto H, Tatsumi K. Cyclic quaternary ammonium ionic liquids with perfluoroalkyltrifluoroborates: synthesis, characterization, and properties. *Chem Eur J*. 2006;12:2196–2212.
37. Zhou ZB, Matsumoto H, Tatsumi K. Structure and properties of new ionic liquids based on alkyl- and alkenyltrifluoroborates. *ChemPhysChem*. 2005;6:1324–1332.
38. Branco LC, Rosa JN, Ramos JJM, Afonso CAM. Preparation and characterization of new room temperature ionic liquids. *Chem Eur J*. 2002;8:3671–3677.
39. Bonhôte P, Dias A, Papageorgiou N, Kalyanasundaram K, Gratzel M. Hydrophobic, highly conductive ambient-temperature molten salts. *Inorg Chem*. 1996;35:1168–1178.
40. Matsumoto H, Sakaebe H, Tatsumi K. Preparation of room temperature ionic liquids based on aliphatic onium cations and asymmetric amide anions and their electrochemical properties as a lithium battery electrolyte. *J Power Sources*. 2005;146:45–50.
41. Hagiwara R, Ito Y. Room temperature ionic liquids of alkylimidazolium cations and fluoroanions. *J Fluor Chem*. 2000;105:221–227.
42. Kulkarni PS, Branco LC, Crespo JG, Nunes MC, Raymundo A, Afonso CAM. Comparison of physicochemical properties of new ionic liquids based on imidazolium, quaternary ammonium, and guanidinium cations. *Chem Eur J*. 2007;13:8478–8488.
43. Zhou ZB, Matsumoto H, Tatsumi K. Low-melting, low-viscous, hydrophobic ionic liquids: 1-alkyl(alkylether)-3-methylimidazolium perfluoroalkyltrifluoroborate. *Chem Eur J*. 2004;10:6581–6591.
44. Tsunashima K, Sugiya M. Physical and electrochemical properties of low-viscosity phosphonium ionic liquids as potential electrolytes. *Electrochem Commun*. 2007;9:2353–2358.
45. Zhou ZB, Matsumoto H, Tatsumi K. Low-melting, low-viscous, hydrophobic ionic liquids: aliphatic quaternary ammonium salts with perfluoroalkyltrifluoroborates. *Chem Eur J*. 2005;11:752–756.
46. Le MLP, Alloin F, Strobel P, Leprêtre JCL, del Valle CP, Judeinstein P. Structure-properties relationships of lithium electrolytes based on ionic liquid. *J Phys Chem B* 2010;114:894–903.
47. Matsumoto H, Kageyama H, Miyazaki Y. Room temperature ionic liquids based on small aliphatic ammonium cations and asymmetric amide anions. *Chem Commun*. 2002;1726–1727.
48. Crosthwaite JM, Muldoon MJ, Dixon JK, Anderson JL, Brennecke JF. Phase transition and decomposition temperatures, heat capacities and viscosities of pyridinium ionic liquids. *J Chem Thermodyn*. 2005;37:559–568.
49. Yoshida Y, Kondo M, Saito G. Ionic liquids formed with polycyano 1,1,3,3-tetracyanoallyl anions: substituent effects of anions on liquid properties. *J Phys Chem B*. 2009;113:8960–8966.
50. Bandrés I, Giner B, Gascón I, Castro M, Lafuente C. Physicochemical characterization of *n*-butyl-3-methylpyridinium dicyanamide ionic liquid. *J Phys Chem B*. 2008;112:12461–12467.
51. McEwen AB, Ngo HL, LeCompte K. Electrochemical properties of imidazolium salt electrolytes for electrochemical capacitor applications. *J Electrochem Soc*. 1999;146:1687–1695.
52. Froba AP, Kremer H, Leipertz A. Density, refractive index, interfacial tension, and viscosity of ionic liquids [EMIM][$EtSO_4$], [EMIM][NTf_2], [EMIM][$N(CN)_2$], and [OMA][NTf_2] in dependence on temperature at atmospheric pressure. *J Phys Chem B*. 2008;112:12420–12430.
53. Okoturo OO, VanderNoot TJ. Temperature dependence of viscosity for room temperature ionic liquids. *J Electroanal Chem*. 2004;568:167–181.
54. Bandrés I, Pera G, Martín S, Castro M, Lafuente C. Thermophysical study of 1-butyl-2-methylpyridinium tetrafluoroborate ionic liquid. *J Phys Chem B*. 2009;113:11936–11942.
55. Chen PY, Hussey CL. Electrodeposition of cesium at mercury electrodes in the tri-1-butylmethylammonium bis((trifluoromethyl)sulfonyl)imide room-temperature ionic liquid. *Electrochim Acta*. 2004;49:5125–5138.
56. Harris KR, Kanakubo M, Woolf LA. Temperature and pressure dependence of the viscosity of the ionic liquids 1-methyl-3-octylimidazolium hexafluorophosphate and 1-methyl-3-octylimidazolium tetrafluoroborate. *J Chem Eng Data*. 2006;51:1161–1167.
57. Harris KR, Woolf LA. Temperature and pressure dependence of the viscosity of the ionic liquid 1-butyl-3-methylimidazolium hexafluorophosphate. *J Chem Eng Data*. 2005;50:1777–1782.
58. Schreiner C, Zugmann S, Hartl R, Gores HJ. Temperature dependence of viscosity and specific conductivity of fluoroborate-based ionic liquids in light of the fractional Walden rule and Angell's fragility concept. *J Chem Eng Data*. 2010;55:4372–4377.
59. Ghatee MH, Zare M, Zolghadr AR, Moosavi F. Temperature dependence of viscosity and relation with the surface tension of ionic liquids. *Fluid Phase Equilib*. 2010;291:188–194.
60. Wang YG, Chen DX, Ou Yang XK. Viscosity calculations for ionic liquid-cosolvent mixtures based on eyring's absolute rate theory and activity coefficient models. *J Chem Eng Data*. 2010;55:4878–4884.
61. Kôddermann T, Ludwig R, Paschek D. On the validity of Stokes–Einstein and Stokes–Einstein–Debye relations in ionic liquids and ionic-liquid mixtures. *ChemPhysChem*. 2008;9:1851–1858.
62. Siqueira LJA, Ribeiro MCC. Alkoxy chain effect on the viscosity of a quaternary ammonium ionic liquid: molecular dynamics simulations. *J Phys Chem B*. 2009;113:1074–1079.
63. Rey-Castro C, Vega LF. Transport properties of the ionic liquid 1-ethyl-3-methylimidazolium chloride from equilibrium molecular dynamics simulation. The effect of temperature. *J Phys Chem B*. 2006;110:14426–14435.
64. Micaelo NM, Baptista AM, Soares CM. Parametrization of 1-butyl-3-methylimidazolium hexafluorophosphate/nitrate ionic liquid for the GROMOS force field. *J Phys Chem B*. 2006;110:14444–14451.
65. Hunt PA. Why does a reduction in hydrogen bonding lead to an increase in viscosity for the 1-butyl-2,3-dimethyl-imidazolium-based ionic liquids? *J Phys Chem B*. 2007;111:4844–4853.
66. Tsuzuki S, Hayamizu K, Seki S. Origin of the low-viscosity of [emim][$(FSO_2)_2N$] ionic liquid and its lithium salt mixture: experimental and theoretical study of self-diffusion coefficients, conductivities, and intermolecular interactions. *J Phys Chem B*. 2010;114:16329–16336.
67. Ma X, Yan L, Wang X, Guo Q, Xia A. Determination of the hydrogen-bonding induced local viscosity enhancement in room temperature ionic liquids via femtosecond time-resolved depleted spontaneous emission. *J Phys Chem A*. 2011;115:7937–7947.
68. Yu GR, Zhang SJ, Zhou GH, Liu XM, Chen XC. Structure, interaction and property of amino-functionalized imidazolium ionic liquids by ab initio calculation and molecular dynamics simulation. *AIChE J*. 2007;53:3210–3221.
69. Yu GR, Chen XC, Asumana C, Zhang SJ, Liu XM, Zhou GH. Vaporization enthalpy and cluster species in gas phase of 1,1,3,3-tetramethylguanidinium-based ionic liquids from computer simulations. *AIChE J*. 2011;57:507–516.
70. Yu GR, Zhang SJ. Insight into the cation-anion interaction in 1,1,3,3-tetramethylguanidinium lactate ionic liquid. *Fluid Phase Equilib*. 2007;255:86–92.
71. Liu XM, Zhou GH, Zhang SJ, Wu GW, Yu GR. Molecular simulation of guanidinium-based ionic liquids. *J Phys Chem B*. 2007;111:5658–5668.
72. Liu XM, Zhou GH, Zhang SJ, Yu GR. Molecular simulations of phosphonium-based ionic liquid. *Mol Simul*. 2010;36:79–86.
73. Merck. The Ionic Liquid Database. Available at: http://pb.merck.de/servlet/PB/menu/1061470/. Accessed April 2010.
74. Dong Q, Muzny CD, Kazakov A, Diky V, Magee JW, Widegren JA, Chirico RD, Marsh KN, Frenkel M. ILThermo: A free-access web database for thermodynamic properties of ionic liquids. *J Chem Eng Data*. 2007;52:1151–1159; Available at: http://ilthermo.boulder.nist.gov/ILThermo/mainmen u.uix.
75. The Beilstein Database. MDL Information System Gmelin. Available at: http://www.Beils-tein.com. Accessed April 2010.
76. Zhang SJ, Sun N, He XZ, Lu XM, Zhang XP. Physical properties of ionic liquids: database and evaluation. *J Phys Chem Ref Data*. 2006;35:1475–1517; Available at: http://159.226.63.140.
77. Seddon KR, Stark A, Torres MJ. Influence of chloride, water, and organic solvents on the physical properties of ionic liquids. *Pure Appl Chem*. 2000;72:2275–2287.
78. Widegren JA, Laesecke A, Magee JW. The effect of dissolved water on the viscosities of hydrophobic room-temperature ionic liquids. *Chem Commun*. 2005;12:1610–1612.

79. Harris KR, Kanakubo M, Woolf LA. Temperature and pressure dependence of the viscosity of the ionic liquids 1-hexyl-3-methylimidazolium hexafluorophosphate and 1-butyl-3-methylimidazolium bis(trifluoromethylsulfonyl)imide. *J Chem Eng Data.* 2007;52:1080–1085.
80. Fannin AA, Floreani DA, King LA, Landers JS, Wilkes JS. Properties of 1,3-dialkylimidazolium chloride-aluminum chloride ionic liquids, Part 2. Phase transitions, densities, electrical conductivities, and viscosities. *J Phys Chem.* 1984;88:2614–2621.
81. Oleinikova A, Bonetti M. The viscosity anomaly near the critical consolute point of the ionic ethylammonium nitrate-*n*-octanol mixture. *J Chem Phys.* 1996;104:3111–3119.
82. Harris KR, Kanakubo M, Woolf LA. Temperature and pressure dependence of the viscosity of the ionic liquid 1-butyl-3-methylimidazolium tetrafluoroborate: viscosity and density relationships in ionic liquids. *J Chem Eng Data.* 2007;52:2425–2430.
83. Frisch MJ, Trucks GW, Schlegel HB, Scuseria GE, Robb MA, Cheeseman JR, Montgomery JA, Vreven JT, Kudin KN, Burant JC, Millam JM, Iyengar SS, Tomasi J, Barone V, Mennucci B, Cossi M, Scalmani G, Rega N, Petersson GA, Nakatsuji H, Hada M, Ehara M, Toyota K, Fukuda R, Hasegawa J, Ishida M, Nakajima T, Honda Y, Kitao O, Nakai H, Klene M, Knox X, Li JE, Hratchian HP, Cross JB, Adamo C, Jaramillo J, Gomperts R, Stratmann RE, Yazyev O, Austin AJ, Cammi R, Pomelli C, Ochterski JW, Ayala PY, Morokuma K, Voth GA, Salvador P, Dannenberg JJ, Zakrzewski VG, Dapprich S, Daniels AD, Strain MC, Farkas O, Malick DK, Rabuck AD, Raghavachari K, Foresman JB, Ortiz JV, Cui Q, Baboul AG, Clifford S, Cioslowski J, Stefanov BB, Liu G, Liashenko A, Piskorz P, Komaromi I, Martin RL, Fox DJ, Keith T, Al-Laham MA, Peng CY, Nanayakkara A, Challacombe M, Gill PMW, Johnson B, Chen W, Wong MW, Gonzalez C, Pople JA. *Gaussian 03, Revision C.01*. Wallingford CT: Gaussian, Inc., 2004.
84. Katritzky AR, Lobanov VS, Karelson M. *CODESSA Reference Manual, Version 2.0*. Shawnee, KS: Copyright © Semichem and the University of Florida 1995–1997, 1996.
85. Randic M. On the characterization of molecular branching. *J Am Chem Soc.* 1975;97:6609–6615.
86. Xue CX, Zhang RS, Liu HX, Liu MC, Hu ZD, Fan BT. Support vector machines-based quantitative structure-property relationship for the prediction of heat capacity. *J Chem Inf Comput Sci.* 2004;44:267–274.
87. Stanton DT, Jurs PC. Development and use of charged partial surface area structural descriptors in computer-assisted quantitative structure-property relationship studies. *Anal Chem.* 1990;62:2323–2329.
88. Katritzky AR, Petrukhin R, Jain R, Karelson M. QSPR analysis of flash points. *J Chem Inf Comput Sci.* 2001;41:1521–1530.
89. Jover J, Bosque R, Sales J. Determination of abraham solute parameters from molecular structure. *J Chem Inf Comput Sci.* 2004;44:1098–1106.
90. Bosque R, Sales J. A QSPR study of the *p* solute polarity parameter to estimate retention in HPLC. *J Chem Inf Comput Sci.* 2003;43:1240–1247.
91. Yuan YN, Zhang RS, Hu RJ. Prediction of photolysis of PCDD/Fs adsorbed to spruce [*Picea abies* (L.) Karst.] needle surfaces under sunlight irradiation based on projection pursuit regression. *QSAR Comb Sci.* 2009;28:155–162.
92. Li J, Liu H, Yao XJ, Liu MC, Hu ZD, Fan BT. Structure–activity relationship study of oxindole-based inhibitors of cyclin-dependent kinases based on least-squares support vector machines. *Anal Chim Acta.* 2007;581:333–342.
93. Luan F, Liu HT, Gao Y, Guo L, Zhang XY, Guo Y. A quantitative structure-activity relationship study of some commercially available cephalosporins. *QSAR Comb Sci.* 2009;28:1003–1009.
94. Takkis K, Sild S, Maran U. The QSAR modeling of cytotoxicity on anthraquinones. *QSAR Comb Sci.* 2009;28:829–833.
95. Basak SC, Harriss DK, Magnuson VR. Comparative study of lipophilicity versus topological molecular descriptors in biological correlations. *J Pharm Sci.* 1984;73:429–434.
96. Suzuki T, Ebert R, Schuurmann G. Development of both linear and nonlinear methods to predict the liquid viscosity at 20°C of organic compounds. *J Chem Inf Comput Sci.* 1997;37:1122–1128.
97. Rajappan R, Shingade PD, Natarajan R, Jayaraman VK. Quantitative structure-property relationship (QSPR) prediction of liquid viscosities of pure organic compounds employing random forest regression. *Ind Eng Chem Res.* 2009;48:9708–9712.
98. Katritzky AR, Chen K, Wang Y, Karelson M, Lucic B, Trinajstic N, Suzuki T, Schuurmann G. Prediction of liquid viscosity for organic compounds by a quantitative structure-property relationship. *J Phys Org Chem.* 2000;13:80–86.

Manuscript received May 25, 2011, and revision received Sept. 20, 2011.